Search for Parity Mixing in $17/2^-$ Isomer of ^{93}Tc

B.A. Brown, F.M. Bernthal, R.A. Warner, and L.E. Young

In work recently published,[1] it was discovered that a $17/2^-$ isomeric level at 2185 keV in ^{93}Tc lies 0.44 ± 0.02 keV above a rapidly decaying $17/2^+$ level (see Fig. 1). This near degeneracy suggested the possibility of observing a significant parity admixture in the $17/2^-$ level since the admixed amplitude for a given parity-non-conserving matrix element is increased by a small energy denominator. From a calculated value for $B(E2)[17/2^+ \rightarrow 13/2^+] = 114\ e^2fm^4$ and from the experimental branching ratios, a limit for the parity-non-conserving matrix element was found to be

$$|\langle 17/2^+| H_{PN} |17/2^-\rangle| \leq 0.34 \text{ eV}.$$

As this limit is of the same order of magnitude as theoretical estimates[2] and is smaller than the result, $|\langle H_{PN}\rangle| = 0.90 \pm 0.45$ eV, obtained by Adelberger et al.[3] for the $J = 1/2$ states in ^{19}F, experiments were designed to measure internal conversion coefficients for the 750.7-keV transition from the $17/2^-$ isomer.

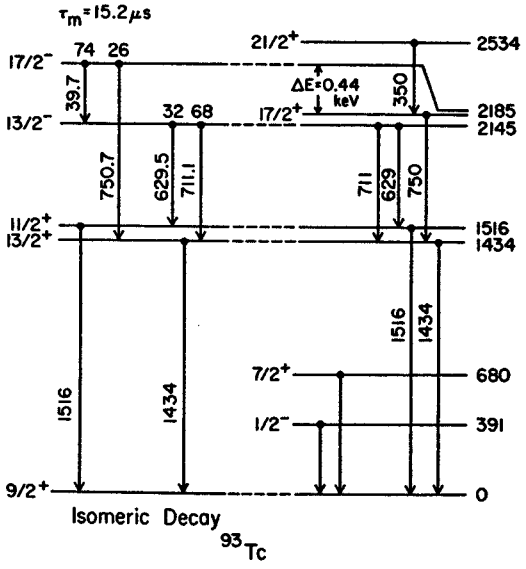

Fig. 1 Scheme of ^{93}Tc levels populated by the $(^6Li, 3n)$ reaction--from Ref. 1. The isomeric decay is indicated on the left hand side.

Ge(Li) γ-ray spectra and electron spectra from the MSU on-line conversion-electron spectrometer[4] were accumulated independently and simultaneously for prompt and several delayed time intervals measured with respect to pulses from the cyclotron beam pulsing system.[5] A simplified diagram of the electronics is displayed in Fig. 2.

The reactions $^{92}Mo(\alpha,p2n)$ at $E_\alpha = 43$ MeV and $^{94}Mo(p,2n)$ at $E_p = 25$ MeV were used. The transitions of interest are far more prominent in the $(\alpha,p2n)$ data. Spectra from this reaction are shown in Fig. 3.

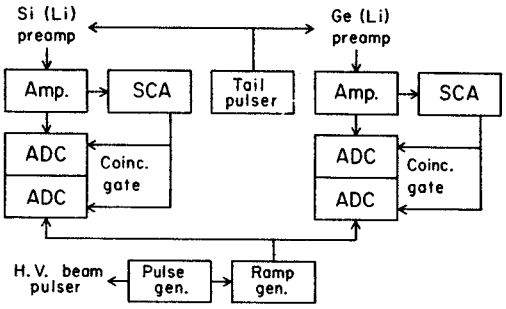

Fig. 2 Simplified diagram of electronics used to accumulate 2-parameter spectra (energy vs. time) for both electrons and γ-rays. The pulse generator is used for dead-time corrections.

Several experimental conversion coefficients derived from these data are listed in Table 1. A ^{166m}Ho source is used for determination of the energy dependence of the Ge(Li) efficiency, and the efficiency of the electron spectrometer was flattened by cyclically sweeping the current in the solenoid through a range liberally encompassing the momenta of interest. The electron spectrometer efficiency was obtained with a ^{206}Bi source and the theoretical value of $\alpha_K(E2) = 8.11 \times 10^{-3}$ for the 803.1-keV E2 transition in ^{206}Bi was used for an absolute normalization with the Ge(Li) detector. The theoretical coefficients are calculated with the code CATAR of Pauli and Raff.[6] Table 2 compares the experimental results for the 750.7-keV isomeric transition with CATAR[6] calculations for pure E2, M2, and E3 transitions.

The implications of this result for possible parity mixing in the $J = 17/2$ doublet are being studied.

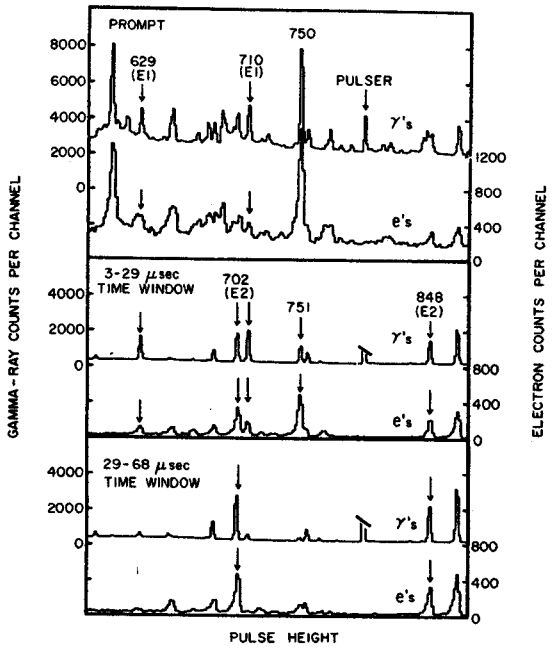

Fig. 3 Prompt and delayed spectra of γ-rays and electrons emitted following the ^{92}Mo(α,p2n) reaction at E_α = 43 MeV.

Table 1 Several K-shell Internal Conversion Coefficients

E_γ (keV)	Assignment & Character	$10^3 \times \alpha_K$ EXP	TH[a]	EXP/TH
	^{93}Tc PROMPT			
750.3	$17/2^+ \rightarrow 13/2^+$	1.40±0.06	1.45	0.96±0.04
	^{93}Tc DELAYED			
750.7	$17/2^- \rightarrow 13/2^+$	3.3 ±0.2	[b]	
711.1	$13/2^- \rightarrow 13/2^+$	0.66±0.03[c]	0.63	1.06±0.05[c]
629.5	$13/2^- \rightarrow 11/2^+$	0.93±0.06[c]	0.82	1.14±0.07[c]
	^{94}Mo DELAYED			
847.7	$6^+ \rightarrow 4^+$	0.98±0.02	1.00	0.98±0.02
702.4	$4^+ \rightarrow 2^+$	1.65±0.03	1.61	1.02±0.02

[a]Calculated with CATAR (Ref. 6).

[b]See Table 2

[c]Complete analysis may increase these errors.

Table 2 K-shell Internal Conversion Coefficient for Isomeric 750.7-keV Transition in ^{93}Tc

α_K(EXP)	Multipolarity	α_K(TH)[a]
$(3.3\pm0.2)\times10^{-3}$	E2	1.450×10^{-3}
	M2	3.921×10^{-3}
	E3	3.363×10^{-3}

[a]Calculated with CATAR (Ref. 6).

REFERENCES

1. B.A. Brown, D.B. Fossan, P.M.S. Lesser, and A.R. Poletti, Phys. Rev. C13, 1194 (1976).
2. M. Gari, Physica Reports 6C, 319 (1973).
3. E.G. Adelberger, H.E. Swanson, M.D. Cooper, J.W. Tape, and T.A. Trainor, Phys. Rev. Letters 34, 402 (1975).
4. See description in the instrumentation section of this report.
5. J.F.P. Marchand and T.L. Khoo, MSU Cyclotron Annual Report 1973-74, p. 80.
6. H.C. Pauli and U. Raff, Computer Physics Comm. 9, 392 (1975).

High Angular Momentum States in ^{118}Sb

W.H. Bentley, R.A. Warner, Wm.C. McHarris and W.H. Kelly

The study of the excited states of ^{118}Sb via the (p,nγ) reaction has been extended to include the (^{7}Li, 3nγ) reaction using the tandem Van de Graaff acclerator at the University of Notre Dame. The purpose of these experiments is to study the high spin structure of ^{118}Sb and in so doing perhaps determine if this nucleus exhibits deformations at high angular momentum. The earlier studies of ^{118}Sb[1] were performed using the reaction $^{118}Sn(p,n\gamma)^{118}Sb$ which populates mostly the low angular momentum states. With the ^{114}Cd (^{7}Li, 3nγ) reaction, large amounts of angular momentum are transferred. The experiments performed consisted of an excitation function measurement and a gamma-gamma coincidence.

The excitation function data were taken in 2 MeV steps from 22 MeV to 30 MeV. Using these data individual gamma-rays can be identified as belonging to ^{118}Sb. In addition, from the shapes of individual gamma-ray excitation functions, a crude estimate can be made of the relative spins of levels depopulated by the gamma rays. The gamma-gamma coincidence experiment was performed at 26 MeV. These data also aided in identifying gamma-rays and were used in constucting a decay scheme.

Shown in Fig. 1 is a tentative decay scheme that is the result of a preliminary analysis of the data. A comparison of the present results with those obtained earlier using the (p,nγ) reaction, gives almost complete agreement for the low lying levels and gamma-rays. The levels which appear in the analysis of the data of the two reactions are given in Table 1. Many of the remaining higher energy states populated by the (p,nγ) reaction are not found in the more recent heavy ion data. However, additional high angular momentum states were excited, allowing identification of 23 gamma-rays and 19 levels previously unseen.

One still unanswered question remaining from the (p,nγ) studies is: does the 273.9 keV gamma-ray decay to ground? This gamma-ray could possibly decay to either the 30.9 or 50.8 keV levels. The present data do not distinguish between these possibilities. Consequently the "273.9 keV level" and all of the levels built on it, including the 19 new levels, may possible lie 30.9 or 50.8 keV higher than shown. Also worth noting is that the 264.4 keV level has no gamma-ray transitions which depopulate it. This indicates a possible interpretation of this level as the $J^{\pi}=8^{-}$, 5.1-hour isomer. If this is correct, the level β-decays to ^{118}Sn and there is no gamma-ray de-excitation to lower levels. Also interesting to note are the three gamma-rays which form a cascade built on the 1404.3keV level. Their energies, 387.3,361.9, and 326.3 keV, correspond quite well to the energy differences in a rotational band following the I(I+1) rule. If the 1404 keV state has J=10, the three transitions may be fitted to a rotational structure resulting in an average rotational constant of 14.9 keV. This may be an indication of the existence of a deformation in the high angular momentum states of this nucleus close to the Z=50 shell.

We wish to acknowledge J.W. Mihelich, E.G. Funk and F. Venezia of the physics department at the University of Notre Dame for their assitance in performing these experiments.

Table 1--Comparison of the levels populated in the (p,nγ) and (^{7}Li, 3nγ) studies. In those cases where levels are seen in both reactions, energies from the (p,nγ) studies were adopted.

(p,nγ)	(^{7}Li,3nγ)	(p,nγ)	(^{7}Li,3nγ)
30.9	30.9	938.2	
50.8	50.8	940.0	
81.6	81.6		941.6
165.7	165.7		945.2
	264.4		979.2
269.4	269.4	984.8	
273.9	273.9	998.1	
324.0	324.0	1016.2	
397.7	397.7	1018.8	
403.2	403.2	1025.2	
506.7			1031.0
507.7		1043.7	
540.3	540.3	1072.5	
556.8	556.8	1093.9	
568.2	568.2	1095.8	
	577.2	1116.8	
	582.6	1130.5	
621.9		1153.6	
628.6		1159.7	
637.2	637.2		1201.6
682.6	682.6	1213.1	
740.9			1350.1
	786.5		1404.3
788.2			1724.9
	801.6		1730.6
833.2			2092.5
	836.4		2117.1
863.2			2479.8
	904.2		

REFERENCES

1. MSUCL Annual Report, 1972-73, p. 52.

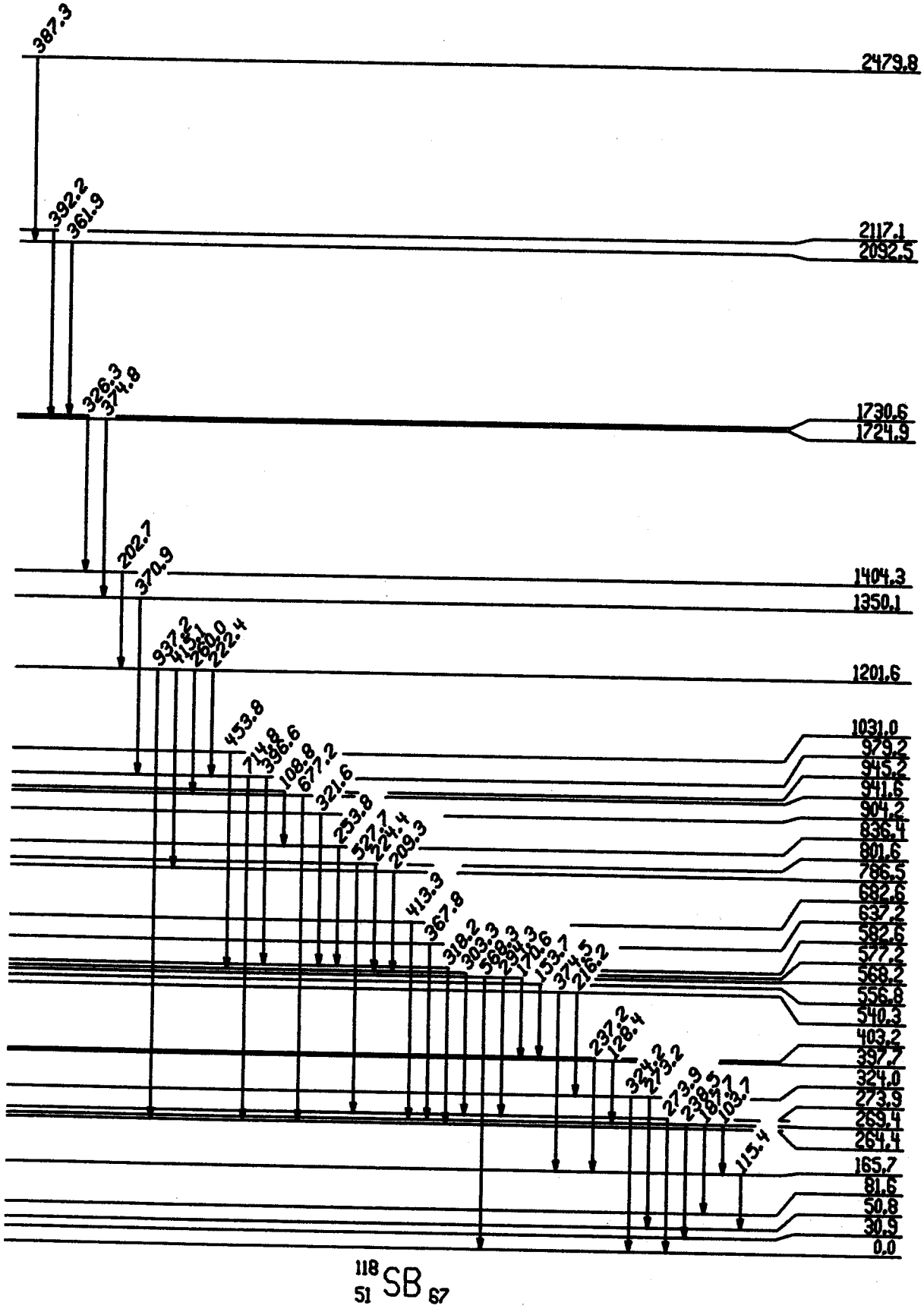

FIG. 1.--Tentative and partial energy level diagram of $^{118}_{51}Sb$.

Structural Changes in the Yrast Levels of ^{178}Hf

T.L. Khoo and G. Løvhøiden*

The high spin structure of ^{178}Hf has been determined from γ-ray studies using the (α,2n) reaction, with α-beams at MSU and also at McMaster University. As shown in Fig. 1, the ground state band and two $K^\pi=8^-$ bands have been identified. Also indicated in the figure is a 4-quasiparticle $K^\pi=16^+$ state[1,2], a 31 year isomer[1] at ∿2.4 MeV.

It is interesting to note that the 12^+ member of the ground state band lies higher than the 12^- member of the lower $K^\pi=8^-$ band. Hence, for $I \geq 12$ the ground band is no longer the yrast sequence; this is now formed by the lower $K^\pi=8^-$ band. A second switch in the yrast character occurs at I=16, when the 31 year isomer (and presumable its associated band) now constitute the yrast sequence. These features demonstrate that at high spin the least energetic structures are not necessarily associated with collective rotation (ground band) but may instead involve the motion of only a few nucleons. Under these circumstances one may obtain yrast traps. The 31 year isomer is certainly a dramatic one!

Whereas angular momentum associated with collective rotation arises from the motion of many nucleons, with the rotation vector perpendicular to the symmetry axis, the spin in the $K^\pi=16^+$ state is generated by alignment of the four individual nucleon spins along the symmetry axis. At ultra-high spin values, when some nuclei may become oblate[3], the angular momentum of yrast states is also expected[3] to arise from a similar alignment of few nucleon spins along the symmetry axis. Yrast traps[3] may also occur in this case.

Another interesting feature of the ^{178}Hf structure is the identification of the upper $K^\pi=8^-$ band. It has been known[1,4] for some time that the two 8^- bands have mixed proton-neutron 2-qp configurations. The observation of the second upper band and the direct decay of its members to the lower band provide another signature of this configuration admixture. The anomalous decay via interband transitions instead of the normal intraband deexcitations can in fact be quantitively accounted for with a 66-34% mixing ratio. If there were no mixing, direct transitions between proton and neutron 2-qp structures would be severely retarded. Knowledge of the off-diagonal matrix elements have been previously extracted[5,6] to yield information on the residual n-p interaction for deformed nuclei.

References

1. R.G. Helmer and C.W. Reich, Nucl. Phys. A114, 649(1968) and A211, 1(1973).
2. F.W.N. de Boer et al., preprint (1976) IKO, Amsterdam
3. A. Bohr and B.R. Mottelson, Physica Scripta 10A, 13(1974).
4. C.J. Gallagher, Jr. and H.L. Nielsen, Phys. Rev. 126, 1520(1962).
5. H. Massmann et al., Phys. Rev. C9, 2312(1974).
6. T.L. Khoo and G.F. Bertsch, MSU Cyclotron Annual Lab. Report 1972-73, p. 8.

*University of Bergen and McMaster University.

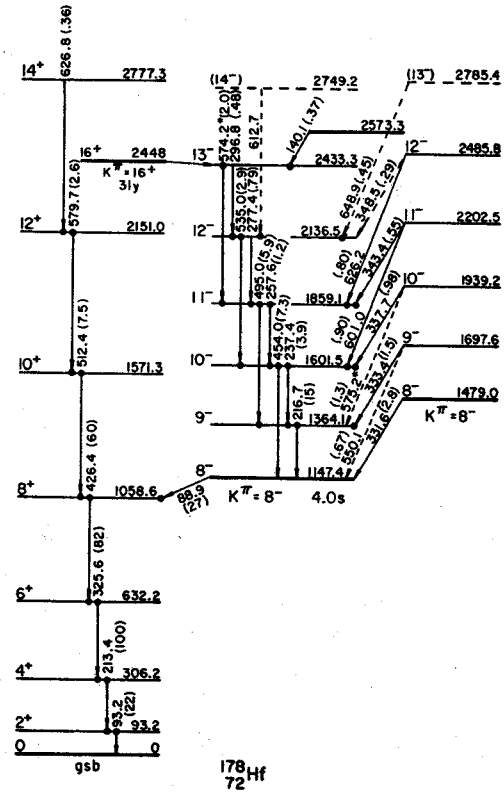

Figure 1: Partial level scheme of ^{178}Hf. Note that the yrast structure changes from the ground band to the members of the $K^\pi=8^-$ and again to $K^\pi=16^+$ state.

High-Spin States in $^{146,147,148,149}Sm$

B.A. Brown, T.L. Khoo, and C.H. King

One challenging open problem in nuclear physics is the determination of the structure of nuclei in regions of transition between spherical and well-deformed shapes. The samarium nuclides have long been of interest in this regard, and the abrupt change of the ground-state shapes between the spherical ^{150}Sm and the prolate deformed ^{152}Sm is well documented. In addition the existence of an excited deformed state in ^{150}Sm and of an excited spherical state in ^{152}Sm has been determined.[1]

The samarium nuclides lighter than ^{150}Sm are believed to be spherical in their ground states. However, those nuclides between ^{150}Sm and the closed neutron shell at ^{144}Sm should be reasonably soft. Thus, in the semiclassical liquid drop picure, as one adds angular momentum to the system, one might expect some oblate deformation to set in. Calculations[2] have indicated that oblate deformations may occur at very low spin ($I<10\hbar$) in ^{146}Sm. The existence of these oblate shapes is of particular interest because they may lead to isomeric states ("yrast traps"), as has been predicted by Bohr and Mottelson.[3] On the other hand, it is possible that unless one gets to very high angular momentum values, most of the angular momentum will go into spherical intrinsic excitations.

To test these ideas we have examined states in the nuclides $^{146,147,148,149}Sm$. We have utilized the $^{146,148}Nd$ $(\alpha,xn\gamma)$ reactions, making γ-γ coincidence, γ-singles angular distributions and excitation function measurements. These reactions should excite states in the final nuclei up to about 20 $\hbar$. In addition, in collabaration with the nuclear-chemistry group at ORNL, we have taken γ-γ coincidence data for the reaction $^{130}Te(^{22}Ne,6n\gamma)^{146}Sm$.

The data analysis is still in a preliminary stage. Nevertheless, the initial indications are that γ-transitions from states up to 6 MeV in excitation have been observed with spins up to about 16 $\hbar$. However, no indications have been found for the existence of rotational structures, and it seems likely that most of the angular momentum is of a spherical intrinsic character, coming from the high-angular-momentum single-particle orbits in this mass region. An attempt to understand our results from the viewpoint of the weak-coupling model is planned.

REFERENCES

1. J.H. Bjerregaard, O. Hansen, O. Nathan, and S. Hinds, Nucl. Phys. 86 (1966) 145.

2. R. Bengtsson, et al., Phys. Lett. 57B (1975) 301.

3. A. Bohr and B.R. Mottelson, Physica Scripta 10A (1974) 13.

High-Spin Multi-Quasiparticle States in Even Hf and W Nuclei

T.L. Khoo, F.M. Bernthal, S.R. Faber, R.G.H. Robertson and R.A. Warner

The Hf and W region is a particulary fruitful area for the study of high-K multi-quasiparitcle (qp) states because of the predominance of high-Ω orbitals. Our interest in high-K states is motivated by the following considerations. (1) Information on the residual nucleon interaction may be extracted from the energies of 4-qp states and their constituent 2-qp structures. This is discussed in ref. 1 and will not be treated here. (2) The applicability of the collective model in a region of excitation (2-5 MeV) never previously investigated in detail may be tested. (3) The role of few-particle motion in nuclear behavior at high-spin, particularly its competition with collective motion, may be delineated. (4) The relationship with spin for the energy expanded in generating angular momentum by nucleon alignment may be explored by identifying intrinsic states over a wide range of spin. The last two points are of relevance to the study of nuclei at ultra-high spins (30-100 ħ), a field which is beginning to generate considerable interest.

The nuclei we are studying are ^{174,176,178}Hf and ^{178,180,182}W. Results on ^{178}Hf and ^{178,182}W are covered elsewhere in this report. The main features of ^{174}Hf are described in the 1973/74 Annual Report. The half-life of the $K^\pi=6^+$ isomer has since been determined to be 133 nsec, instead of the 2.1 μsec value previously reported by Ejiri et al.[2] The erroneous value was probably due to feeding from the 2.4 μsec $K^\pi=8^-$ isomer. In ^{180}W we have identified the rotational band built on the previously known[3] 5.2 msec $K^\pi=8^-$ isomer. The band is fed by a 4-qp isomer with a ≈3 μsec half-life. The study on ^{176}Hf is complete and subsequent discussion will be confined to it.

Fig. 1 shows the high-spin levels in ^{176}Hf, which include the upper portion of the ground band; three 4-qp states, two with well-behaved rotational bands; and three 6-qp states. The proposed configurations for the states are given in Table 1.

The 6-qp states and the 4-qp rotational bands are observed for the first time. Indeed, there are more high-spin states here than have been identified in any other nucleus. The 22^- isomer is the highest spin isomer observed to date. The properties of these highly excited intrinsic states are well described by the collective model, indicating that there is no break-down of this model at energies between 2.5 and 5 MeV. In particular, K appears to remain a good quantum number (at least for large K-values), as is also illustrated by the K-forbidden isomerism of the $K^\pi=14^-$ and 19^+ band-heads. Thus, axial symmetry is preserved.

Inspection of Fig. 1 reveals that the $K^\pi=16^+$ band-head lies lower than the 16^+ state of the ground band. The yrast structure thus switches character for $I \geq 16$ from the ground band to the members of the $K^\pi=16^+$ band. A further change occurs at spin 22 when the I $K^\pi=22$ 22^- state becomes yrast. Structural changes in the yrast line also occur in ^{178}Hf[4]. This demonstrates vividly that the energetically favoured states at high-spin do not necessarily arise from collective rotations (ground band) but may instead be associated with few-nucleon structures.

The dominance of high-K multi-qp structures along or near the yrast line for $I \gtrsim 16$ has important implications for the electromagnetic decay of the yrast states. For instance, the 22^- and 16^+ yrast levels de-excite not by collectively enhanced stretched E2 transitions but by slower single-particle transitions. Thus, the 22^- isomer at almost 5 MeV is a yrast trap, while the $K^\pi=19^+$ and 14^- isomers are traps which occur very close to the yrast line. There are many similarities between these traps and those which have been predicted[5,6] to occur at ultra-high spin values, when some nuclei are expected to become oblate. Both cases involve the motion of a few nucleons around the symmetry axis; the large spin generated by alignment of nucleon orbits thus lies along the symmetry axis. (Most of the orbits of present interest have large Ω. Thus the particle trajectories are concentrated near the equatorial plane, and involve revolutions around the nuclear symmetry axis.) In contrast, the spin in collective rotation is perpendicular to the symmetry axis.

Bohr and Mottelson[5,6] have recently shown that the energy expended in generating angular momentum by alignment of particle orbits has a rotation-like relationship with spin. Furthermore the effective moment of inertia is that for rigid body rotation about the axis around which the nucleons move. A plot of the energies of the lowest band-head of each spin in ^{176}Hf as a function of I(I+I) is shown in Fig. 2. The data are distributed about a straight line which represents a moment of inertia $2\ I/\hbar^2 = 130\ \text{MeV}^{-1}$. For rigid body rotation about the symmetry axis of an ellipsoid with $\delta = 0.28$, the ground state deformation, we have $2\ I_3/\hbar^2 = 126\ \text{MeV}^{-1}$, a value close to the above. Although it is tempting to treat the data of Fig. 2 as evidence for the concept[5,6] of a moment of inertia associated with the alignment of single-particle orbits around a symmetry axis, the large effect of pairing

interactions in the configurations considered raises serious questions about such an interpreattion. The near rigid value of the moment of inertia for the band-heads may be fortuitous, perhaps occurring because of the opposing tendencies of pairing effects (which tend to decrease the effective moment of inertia by increasing the intrinsic energies) and shell effects (viz. the predominance of high-Ωorbitals near the Fermi levels, which lowers the energies of high-K states). Nevertheless, the small scatter of the points about the solid straight line of Fig. 2 is quite remarkable and suggests that efforts should be made toward constructing similar plots for other nuclei by identifying high-K qp-states over a wide range of spin.

Although the concept of rotation about a symmatry axis has not been unambiguously demonstrated, many of the other physical concepts introduced by Bohr and Mottelson[5,6] in connection with the behaviour of nuclei in a higher spin domain have found their first demonstration in this study, but at lower spins. For instance, it has been shown that the yrast structure for a deformed nucleus can change from collective rotation to few-nucleon motion; that a few nucleons can then aligh to generate spin along the symmetry axis; and thatyrast traps can occur under these circumstances. This is of significance to the study of nuclei at ultra-high spins.

Table I. Suggested configurations for 4- and 6-qp states observed in ^{176}Hf.

Exp.	Band-head Energy (keV)	Calc.	K^π	Configuration[a]
2866		2838[b]	14^-	$7/2_p 9/2_p 7/2_n 5/2_n$
3080		3190[b]	15^+	$7/2_p 9/2_p 9/2_n 5/2_n$
3266		3061[b]	16^+	$7/2_p 9/2_p 7/2_n 9/2_n$
4377		4600[c]	19^+	$7/2_p 9/2_p 7/2_n 9/2_n$ $5/2_n 1/2_n$
4466		5000[c]	20^-	$7/2_p 9/2_p 7/2_n 9/2_n$ $7/2_n 1/2_n$
4864		5000[c]	22^-	$7/2_p 9/2_p 7/2_n 9/2_n$ $7/2_n 5/2_n$

[a]Single particle orbitals are: $7/2_p$: 7/2(404); $9/2_p$: 9/2(514); $7/2_n$: 7/2(514); $9/2_n$: 9/2(624); $5/2_n$: 5/2(512); $1/2_n$: 1/2(521); $7/2_n$: 7/2(633).

[b]Calculated as described in Ref. 4, using the δ-force given there as the residual interaction.

[c]Estimated from constituent 4- and 2-qp energies, using empirical values when known. Effects of residual interactions and of pairing gap variation due to 2 broken neutron pairs are not properly included in the estimate.

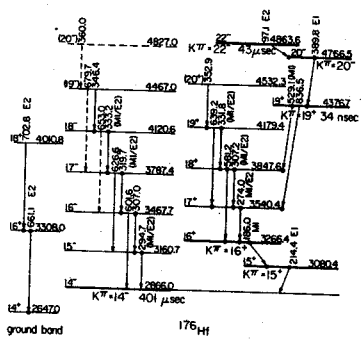

Fig. 1 Partial level scheme for ^{176}Hf showing 4- and 6-qp excitations and upper portion of ground band. Assignments in parentheses are tentative. Filled circles indicate γ-rays entering and leaving a level in prompt coincidence.

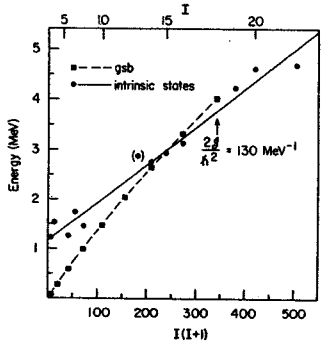

Fig. 2 Plot for ^{176}Hf of lowest band-head energies for given I (circles) and ground band energies (squares) vs I(I+1). For band-heads, zero point energies for rotation about an axis perpendicular to the symmetry axis have been subtracted as described in Ref. 4. Points for intrinsic states are closely distributed about a straight line with slope corresponding to $2I/\hbar^2$=130 MeV^{-1}; for rigid body rotation about the symmetry axis, $2I_3/\hbar^2$=126 MeV^{-1}

REFERENCES

1. T.L. Khoo, F.M. Bernthal, R.A. Warner, G.F. Bertsch and G. Hamilton, Phys. Rev. Lett. 35, 1256(1975).

2. H. Ejiri, S.M. Ferguson, R.H. Heffner and H. Wieman, Radioactivity in Nuclear Spectroscopy, ed. J.H. Hamilton and J.C. Manthuruthil

3. J. Brude et al., Nucl. Phys. 85, 481(1966).

4. T.L. Khoo and G. Løvhøiden this report.

5. A. Bohr and B.R. Mottelson, Physica Scripts 10A, 13(1974).

6. A. Bohr and B.R. Mottelson, Nuclear Structure, v. 2 (Benjamin, New York, 1975), pp. 43-44, 72ff., 80ff.

Multiple Neutron Hole Excitations in Light Odd-A Pb Nuclei

H. Helppi, S.K. Saha, P.J. Daly, S.R. Faber, T.L. Khoo, and F.M. Bernthal

The high-spin level spectra of the semi-magic nuclei ^{203}Pb, ^{201}Pb, ^{199}Pb, ^{197}Pb and ^{195}Pb are being investigated for the first time by means of (α,x$n\gamma$) and (^{3}He, x$n\gamma$) reactions on isotopically enriched Hg targets. Strong yrast cascades "nu" terminating in $\nu i_{13/2}^{-1}$ isomeric states have been observed in all five nuclei. Isotopic identifications have been based on excitation function measurements and on the requirement of intensity balance at all bombarding energies between the transitions populating and depopulating the well established $13/2^+$ isomers. The experiments have included γ-ray singles and comprehensive ($\gamma\gamma t$) coincidence measurements, γ-ray angular distributions and lifetime determinations spanning the range from 2 ns to many seconds. In all of the odd-A Pb nuclei, several new isomers have been located and characterized.

In general, a very close correspondence has been found between the levels built on the $\nu i_{13/2}$ isomer in each of the odd-A nuclei and the high-spin neutron hole excitations previously identified[1,2] in the adjacent even-A Pb core nucleus.

The nucleus ^{203}Pb: A pulsed beam ^{202}Hg(α,3nγ) experiment revealed a ^{203}Pb isomer with $t_{1/2}$ = 0.48 $\pm$ 0.04 sec, which de-excites through high-spin even parity levels to the known 6.2-sec $13/2^+$ isomer at 825 keV. This isomer has also been observed recently by Linden et al.[3] From γ-γ coincidence data and transition multipolarities based on intensity balance requirements, the isomeric decay scheme shown in Figure 1 has been firmly established. The 0.5-sec isomeric state is assigned $J^\pi=29/2^-$; since this state can be attributed to the coupling of the ^{204}Pb 9^- state (Fig. 1) with the additional $\nu i_{13/2}$ hole, the dominant neutron hole configuration $(p_{1/2}^{-2})_{0^+}$, $f_{5/2}^{-1}$, $i_{13/2}^{-2}$, is proposed.

The nuclei ^{201}Pb and ^{199}Pb: These nuclei have been investigated by (α,3nγ) reactions on ^{200}Hg and ^{198}Hg targets. Three new isomeric levels have been identified in each nucleus, as is shown in the simplified level schemes of Fig. 2. The close-lying $17/2^+$, $15/2^+$ and $19/2^+$, $21/2^+$ douplets are almost certainly components of weak coupling multiplets associated with the 2_1^+ and 4_1^+ states of the ^{202}Pb and ^{200}Pb core nuclei. The systematics of the odd parity states also manifest the intrinsic relationship between the prominent high-spin features of the odd-A and even-A level spectra. The change in the odd parity level ordering of both odd-A and even-A isotopes below ^{204}Pb, ^{203}Pb can readily be explained by the location of the Fermi surface (closer to the $p_{3/2}$ subshell than the $f_{5/2}$) in the lighter nuclei.

The nuclei ^{197}Pb and ^{195}Pb: These nuclei have been studied by (^{3}He,4nγ) and (^{3}He,6nγ) reactions on a ^{198}Hg target. In ^{197}Pb, the $21/2^-$ level is isomeric ($t_{1/2}$=1.5 $\pm$ 0.1 μs), and the $17/2^+$, $15/2^+$ and $19/2^+$, $21/2^+$ weak coupling multiplets are again observed (Fig. 2). Our investigation of the ^{195}Pb level structure has not yet been completed, but we have established quite definitely that the 10-μs isomer previously attributed[2] to ^{194}Pb should be re-assigned to ^{195}Pb. Tentatively, we associate the half-life of 10.0 $\pm$ 0.7 μs with the $21/2^-$ level in ^{195}Pt.

The analysis and comtemplation of these results is continuing with particular emphasis on the comparison between modes of excitation and reduced transition probabilities in the odd-A and even-A Pb nuclei.

REFERENCES

1. M. Pautrat et al., Nucl. Phys. A201 (1973) 449 and Physica Scripta 6 (1972) 219.

2. R. Djadali, K. Krien, R.A. Maumann and E.H. Spejewski, Phys. Rev. C8 (1973) 323.

3. C.G. Lindén, I. Bergström and J. Blomquist. Research Institute for Physics, Stockholm, Annual Report (1975) p. 118.

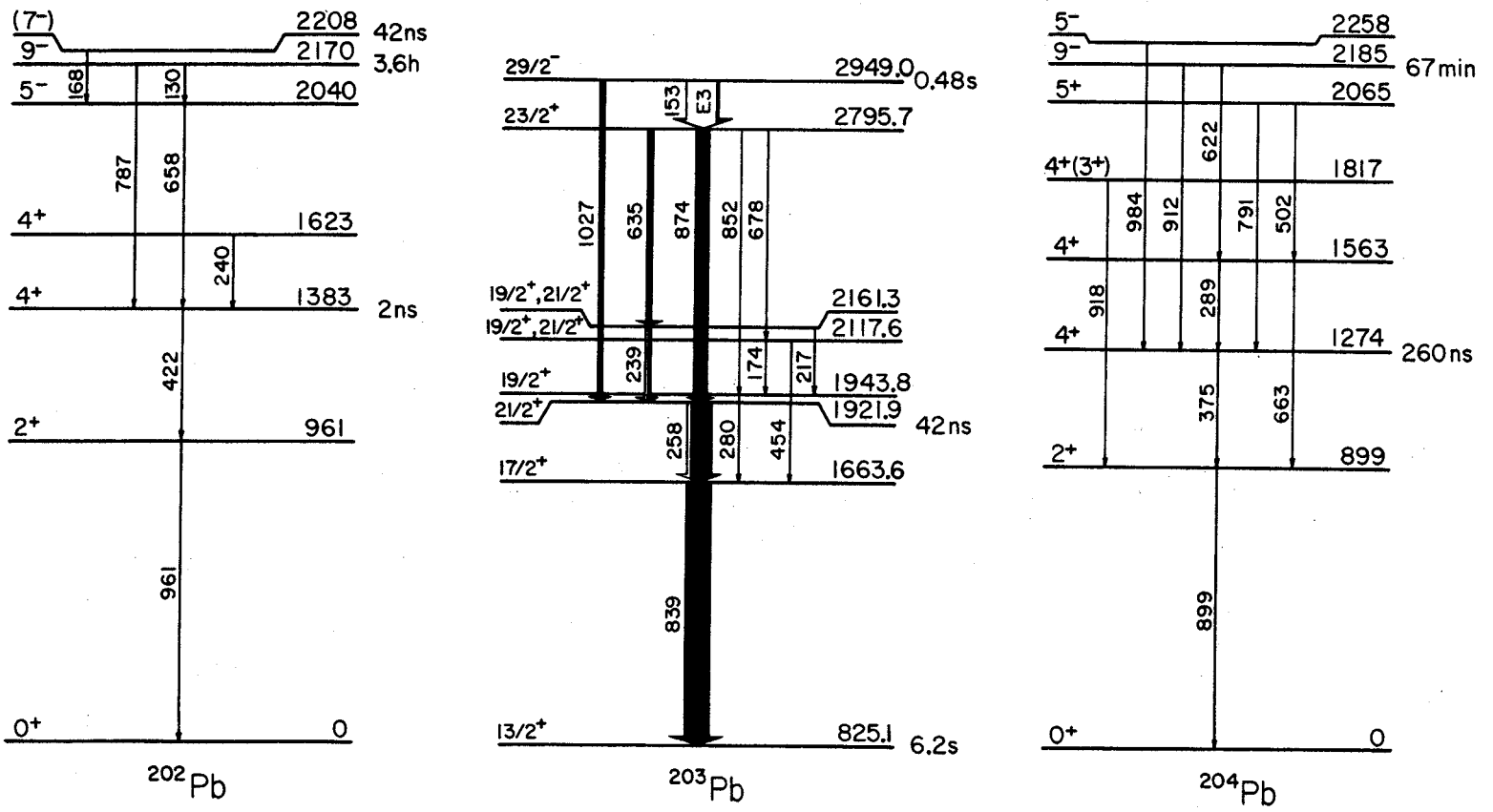

FIG. 1.--Decay scheme of the 0.48-sec isomer in ^{203}Pb. The high-spin level schemes of ^{202}Pb and ^{204}Pb are shown for comparison.

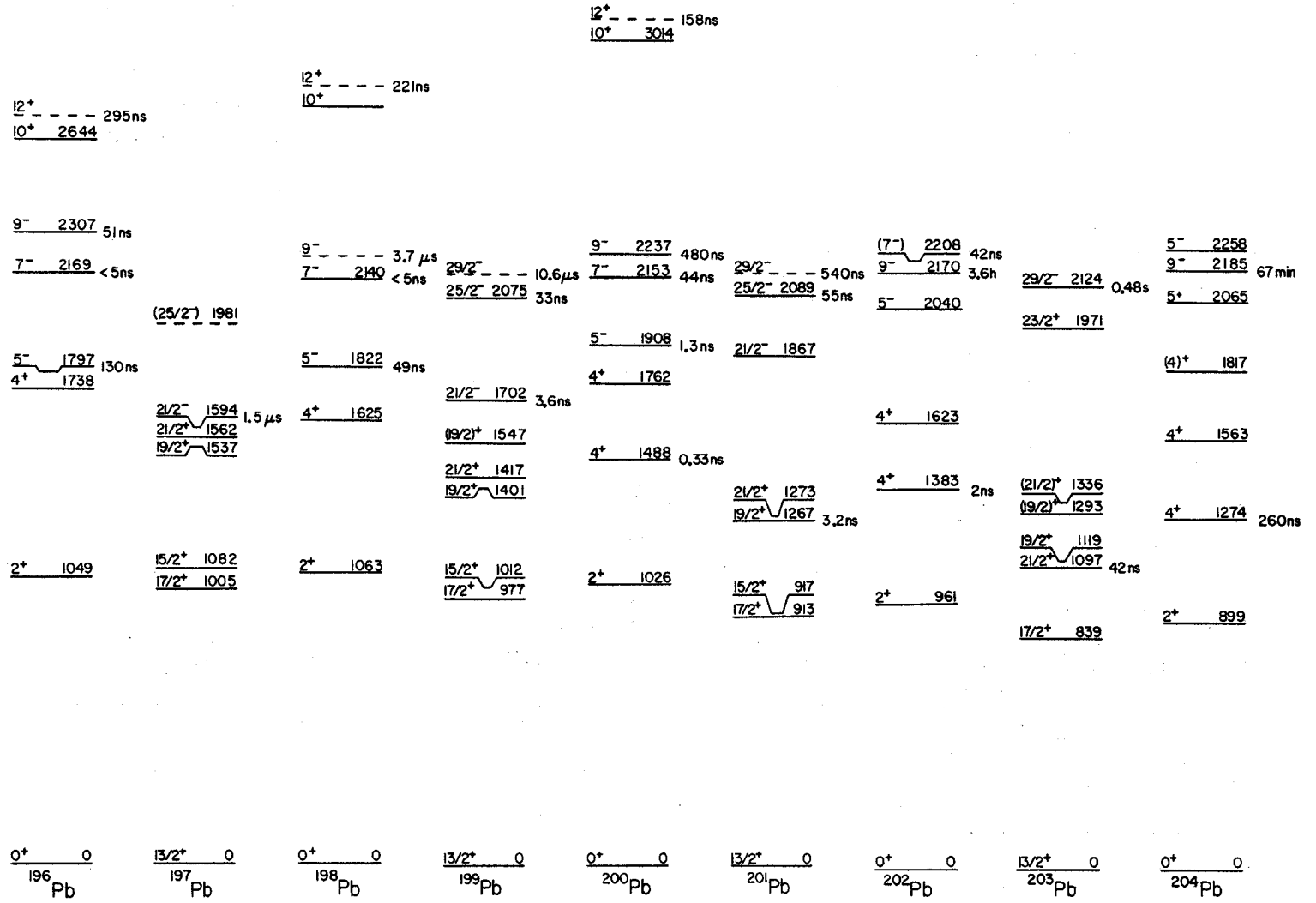

FIG. 2.--High-spin level systematics of $^{196-204}$Pb. The $13/2^+$ isomeric levels in the odd-A nuclei are displaced to zero energy in order to accentuate the resemblance between the odd- and even-A level spectra.

Evidence for Five-Quasiparticle States in ^{177}Ta

L. Buja-Bijunas,* J.C. Waddington,* T.L. Khoo and F.M. Bernthal

A rather thorough study of the high K states in ^{176}Hf has been carried out by Khoo, et al.[1] at McMaster and at Michigan State Universities, and so we have undertaken to do a similar investigation of the neighbouring odd-proton nucleus ^{177}Ta. A group at Grenoble[2] had previously identified various 3-quasiparticle states in ^{177}Ta and a search was begun for other many-quasiparticle states, especially for a 5-quasiparticle state which we believed should exist. Experiments carried out at the Michigan State Cyclotron used the ^{176}Lu(α,3n)^{177}Ta reaction with a beam of 38 MeV α's and a self-supporting target approximately 3 mg/cm^2 thick. This reaction is particularly suitable since the ground state spin of ^{176}Lu is 7^-, thereby making it favourable in populating high spin states.

Figure 1 shows some of the levels populated in this study. The previous study[2] had identified the K=21/2$^-$, 23/2$^+$ and 25/2$^+$ 3-quasiparticle bandheads, the 21/2$^-$ state being isomeric with a half-life of 5 μsec, and had populated states up to 2826.9 keV. The Grenoble group assumed the 2826.9 keV level to be the 33/2$^+$ member of the rotational band built upon the K=25/2$^+$ 3-quasiparticle state. The data we collected showed this level to be actually isomeric in character with a half-life of 70 nsec. In addition, conversion electron data showed the 555 keV transition to be M1 + E2 and the 790 keV transition to be E2. Using this information, we have assigned a spin of 31/2$^+$ to this level instead and propose a 5-quasiparticle configuration, the most favourable being $9/2^-[514]_p$, $1/2^-[521]_n$, $5/2^-[512]_n$, $7/2^-[514]_n$, $9/2^+[624]_n$.

The fact that the 5-quasiparticle state which we are interested in is isomeric is helpful since it makes it possible to use both prompt and delayed coincidence techniques to isolate those transitions which are populating or depopulating the isomer. An example of some of the data collected is shown in Figure 2. The 343 keV transition was gated as the stop signal for coincidences.

The bottom spectrum shows those start events that were in prompt coincidence. The data shows the lines depopulating the isomer. The top spectrum also used the 343 as the stop event but with the restriction that the -rays detected as start signals should preceed the stop signal by a length of time approximately equal to the half-life of the isomer. Because of the delay in time between the two events we know that the initial start γ-rays must populate the isomer. Using this data we have begun to construct the level scheme above the 31/2$^+$ 5-quasiparticle state.

To gain more information about the γ's feeding into the isomer we also sorted out prompt coincidences using transitions above the isomer as the stop signals. The 104, 233 and 322 are only a few of the transitions that have been placed above the 5-quasiparticle isomer. The 104 keV transition has been determined to be E1 in character, but the spins of other high lying states have not yet been definitely determined.

There is still a great deal of information that has not been conclusively sorted and work is presently underway to complete an analysis of the levels above this isomer.

*McMaster University, Hamilton, Canada.

REFERENCES

1. T.L. Khoo, J.C. Waddington, and M.W. Johns, Can. J. Phys. 51,2307(1973); T.L. Khoo, et al., Phys. Rev. Lett. 35,1256(1975). T.L. Khoo, F.M. Bernthal, R.G.H. Robertson and R.A. Warner, submitted for publication.

2. D. Barnéoud, S. André and C. Foin, Phys. Lett. 55B,443(1975).

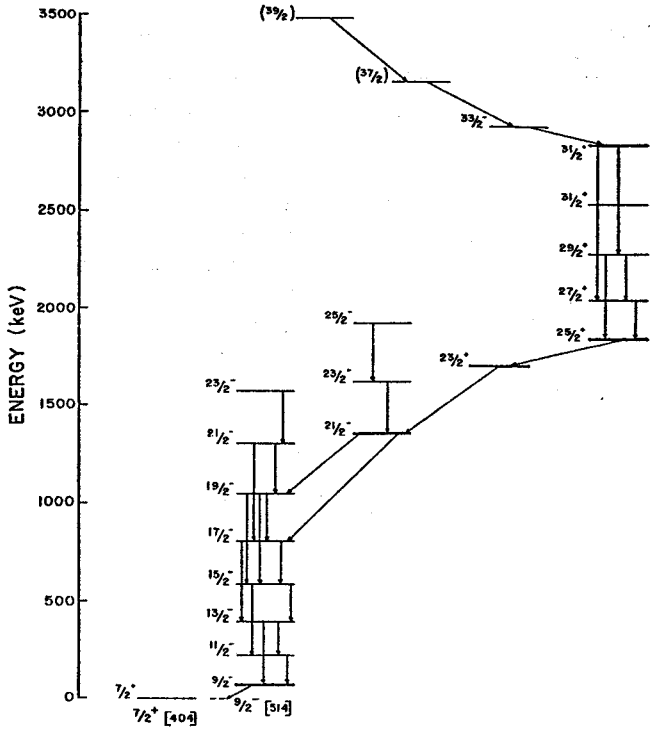

Fig. 1.--Partial level scheme for ^{177}Ta.

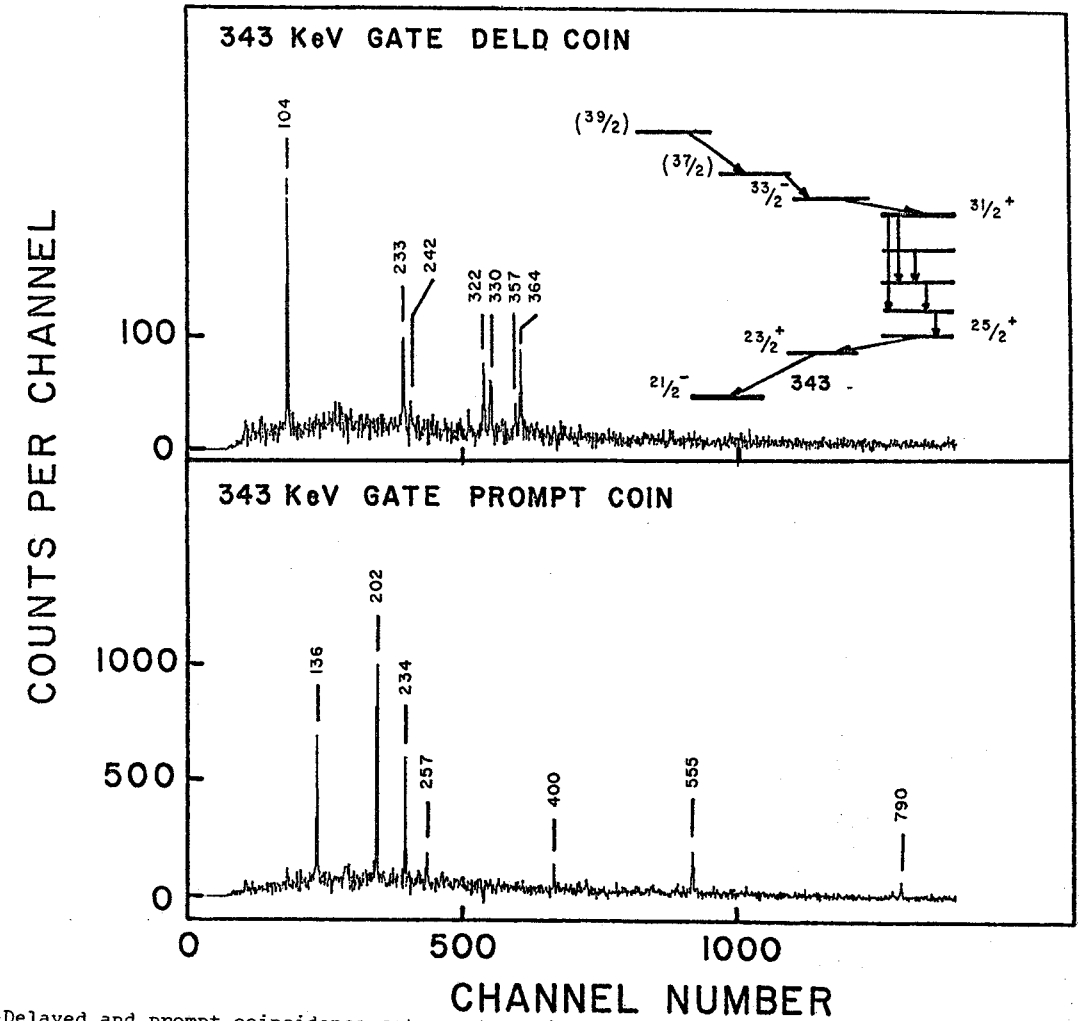

Fig. 2.--Delayed and prompt coincidence gates set on the 343 keV transition. The former shows γ-rays feeding the 33/2⁻ isomer; the latter shows γ-rays de-exciting the same isomer.

Three-Quasiparticle States in ^{177}Hf

I.H. Redmount, T.L. Khoo, and R.A. Warner

A study of gamma-ray and conversion electron spectra of ^{177}Hf revealed three 3-quasiparticle states in that nucleus. In addition to the well-known $K^\pi = 23/2^+$ state, two new 3-quasiparticle states with $K^\pi = 25/2^-$ and $K^\pi = 19/2^-$ were found

The ^{177}Hf was produced via the ^{176}Yb $(\alpha,3n)$ ^{177}Hf reaction, by bombarding ^{176}Yb targets with alpha-particle beams at energies ranging from 34 to 49 MeV. The experiments yielded gamma-ray (singles) spectra, decay time measurements, excitation function and angular distribution data, gamma-gamma coincidence spectra, and conversion electron spectra for delayed transitions.

The one previously known 3-quasiparticle state in ^{177}Hf is the $23/2^+$ $\{7/2(514)_n 7/2(404)_p 9/2(514)_p\}$ isomer, at energy 1315 keV and with half-life 1.1 seconds. One new 3-quasiparticle state identified in these experiments is a $25/2^-$ $\{9/2(624)_n 7/2(404)_p 9/2(514)_p\}$ state at energy 1712 keV. Gamma-gamma coincidence data showed that this state decays via a 120.5 keV transition to the $I^\pi K = 25/2 + 23/2$ state. Examination of angular distribution and electron conversion coefficients established that this transition is E1 and confirmed the $K^\pi = 25/2^-$ assignment for the new state. Several members of the rotational band built on this state were also evident in the gamma spectra. A new three-quasiparticle isomer was found as well, with $K^\pi = (19/2)^-$ and probable configuration $\{7/2(514)_n 7/2(404)_p 5/2(402)_p\}$, at energy 1342 keV. Its half-life was measured to be 55.9 ± 1.2 μsec; the state decays through a 548 keV transition to the $17/2^-$ member of the $K^\pi = 7/2^-$ ground band. Measurements of conversion electron spectra indicate that this transition is an M1/E2 admixture.

The energies of these 2-proton plus odd neutron quasiparticle states may be compared with the energies of the 2-proton quasiparticle states in neighboring even-even Hf nuclei; such comparisons will provide information on the residual nucleon-nucleon interactions.

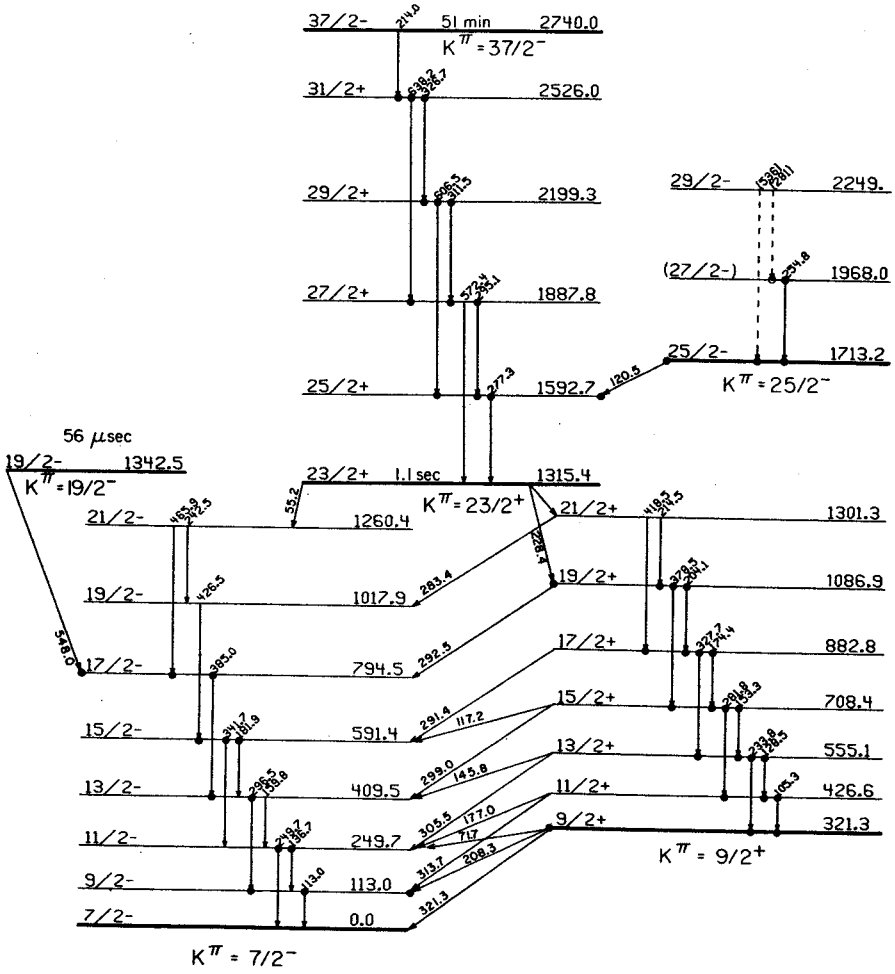

Figure 1: Level Scheme of ^{177}Hf

Excited States of the Odd-Odd Nucleus ^{182}Re

M.F. Slaughter, T.L. Khoo, R.A. Warner, Wm. C. McHarris, and W.H. Kelly

States in ^{182}Re populated by the (α,3n) reaction on a ^{181}Ta foil target are being studied by in-beam 3 parameter prompt and delayed γ-γ coincidence, γ lifetime, and γ angular distribution methods. Coincidence data were taken with 4.5% and 7% Ge(Li) detectors (efficiency given for a 1333 keV-γ relative to a 3" x 3" Na(Tl) detector). Two rotational bands constructed primarily from the coincidence data are shown in Fig. 1.

Gamma-lifetime measurements made with the cyclotron beam sweeper show that the upper band is delayed by 60±4 nsec. By gating off the prompt peak of the TAC spectrum, transitions feeding an isomeric level can be emphasized. Delayed coincidence gates on members of the upper band were summed and an appropriate fraction of the integral coincidence spectrum subtracted to eliminate prompt and chance contamination. From this we infer that the 268.0- and 358.3-keV transitions feed what is probably a four-quasiparticle isomeric level at 2256.6 keV. These two transitions are not in coincidence with each other.

Branching ratios were found from γ singles data taken with a low energy Ge(Li) detector at 125° relative to the beam axis. As a check, ratios for the upper band were also determined from the delayed γ-lifetime data. From the branching ratios values of $|g_K-g_R|/Q_0$ and the mixing ratio δ were calculated. The mixing ratios agreed with those reported by Hjorth, et al.[1] The intrinsic quadrupole moment of ^{182}W (Q_0=6.406) and an assumed value for g_R of 0.3±0.05 were used to find g_K for the two bands. For the ground band we found g_K=0.60±0.12 or 0.00±0.12 and for the upper band, g_K=0.65±0.12 or 0.05±0.12.

We have previously assigned spins of 7^+ and 9^- to the ground state and upper bandhead respectively. A 7^+ ground state is to be expected from the coupling of a $5/2^+[402]$ proton, the odd proton in ^{181}Re, and the $9/2^+[624]$ neutron which lies outside the even-even core in ^{181}W. The 9^- bandhead would result from the coupling of a $9/2^-[514]$ proton to the $9/2^+[624]$ neutron. However, values of g_K calculated for K=7 from the asymptotic expression $g_K=1/K(g_{sp}\Sigma_p\pm g_{sn}\Sigma_n) + g_{lp}\Lambda_{lp}\pm g_{ln}\Lambda_{ln}\}$ with $g_{s,eff}=.6g_{free}$ yield g_K=0.36 which is inconsistent with the experimental value for the lower band. As a check, g_K was calculated using $g_K=1/K\{g_{\Omega p}\Omega_p\pm g_{\Omega n}\Omega_n\}$ with g_Ω determined from the Nilsson wave functions for η=4. This method gave g_K=0.38. Together with some tentative additional evidence from delayed coincidence spectra this result leads us to suspect that the spin assignments may be incorrect and that quite possibly these rotational bands may be built on an excited state. We are currently attempting to resolve these problems.

References

1. S.A. Hjorth, H. Ryde, and B. Skanberg, Arkiv for Fysik 38,29(1968).

2. M.F. Slaughter, et al., MSU Cyclotron Lab Annual Report 1973-1974, pp. 57-58.

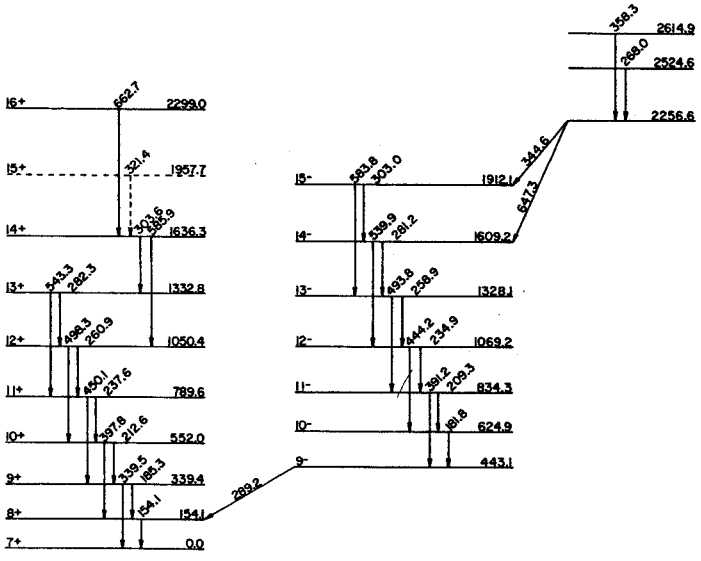

FIG. 1.--Proposed level scheme for ^{182}Re (K assignment may be incorrect as discussed above).

The ε/β^+ Decay of $^{143g+m}$Gd

R.G. Firestone, R.A. Warner, Wm. C. McHarris, and W.H. Kelly

As one example of a decay scheme that adds significant information to the understanding of nuclear structure rather than being just another set of numbers, we outline here the most succinct points of our recent production and study of the new nuclides ^{143m}Gd and ^{143g}Gd. This is a good example of a nucleus far from stability with plenty of decay energy but also close to a major closed shell so that one can make sense and interpret the states seen.

Having completed our work on the decays of ^{143}Sm and ^{143}Eu, we have recently finished studies of the decays of the previously unknown isomers $^{143g+m}$Gd. These nuclei were of interest to us for several reasons. They continue our general studies of N=79 decays to Z=64 and also they give us information concerning the lightest known gadolinium. The latter point is most important because ^{145}Gd was one of the richest nuclei we have yet studied. In these experiments we also make our most extensive use of our HeJRT system [K.L. Kosanke, M.D. Edmiston, R.A. Warner, R.B. Firestone, Wm. C. McHarris, and W.H. Kelly, Nucl. Instr. Meth. 124, 365(1975)] in elucidating information about a nucleus far from the line of β stability.

Sources of $^{143g+m}$Gd were prepared by the ^{144}Sm(^{3}He,4n)$^{143g+m}$Gd reaction on $^{144}Sm_2O_3$ (enriched to 95% ^{144}Sm) pressed oxide targets. Recoils from the target were swept up by a flow of He and delivered to a programmable moving collecting tape where sources were transported to detectors. Transport times were less than 1 sec, but in practice sources were held for 20-30 sec before counting to allow short-lived activity to die away. Counting times were adjusted to maximize the activity of interest over the longer lived daughters and impurities.

In order to characterize $^{143g+m}$Gd, excitation functions were run by degrading 76-MeV ^{3}He beams with an automated absorber unit to 32-76 MeV on target. These excitation functions are shown in Fig. 1. Having found a number of probable candidates for $^{143g+m}$Gd γ-ray transitions, a series of experimental measurements were performed yielding half-life curves. We determined that ^{143g}Gd had a half-life of 39±2 sec and ^{143m}Gd had one of 112±2 sec. Ge(Li)-Ge(Li) megachannel coincidence experiments were then performed to place the remaining γ-rays in either the ^{143m}Gd or ^{143g}Gd decay schemes. Sample coincidence spectra are presented in Fig. 2. From these experiments virtually all of the observed γ-ray transitions could be placed in an appropriate decay scheme. It soon became clear, however, that a level at 389.5 keV in ^{143}Eu was very delayed and would not appear in coincidence. The half-life of this state was measured by pulsed beam techniques to have a half-life of 50.0±0.5 μsec.

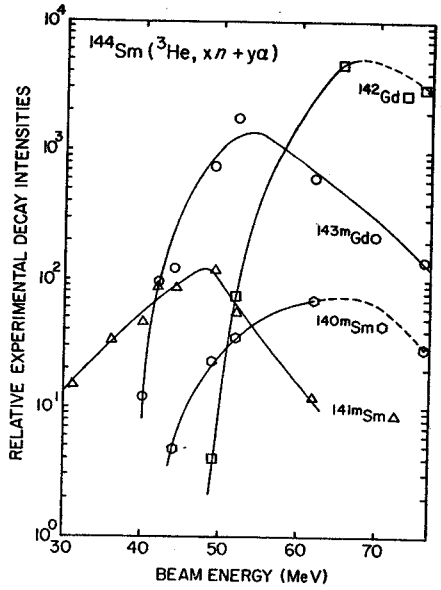

Fig. 1.--Excitation functions for the production of neutron-deficient Gd and Sm isotopes below N=82.

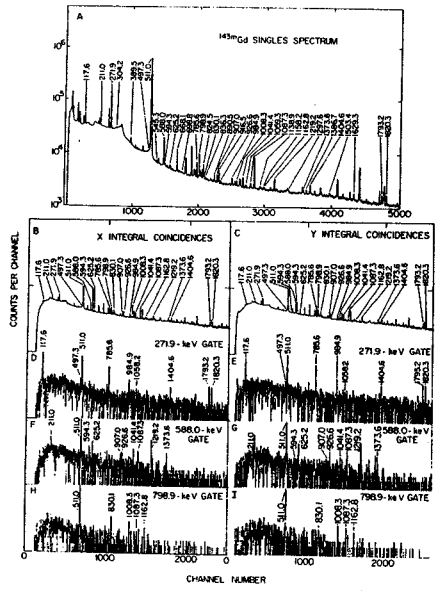

Fig. 2.--Sample megachannel γ-γ coincidence spectra taken in the study of ^{143m}Gd decay.

In Fig. 3 are the resultant decay schemes. The decay energy is a calculated value [W. D. Myers and Swiatecki, Nuclear Masses and Deformations, UCRL-11980, 1965] and the log ft's assume no ground-state feeding. The spin 1/2 assigned to ^{143g}Gd is based on the systematics of the well known neighboring nuclei ^{141g}Sm [R. R. Todd, Ph.D. Thesis, Michigan State University, 1971 (unpublished)] and ^{145g}Gd [R. E. Eppley, Wm. C. McHarris, and W. H. Kelly, Phys. Rev. C3, 282 (1971)]. This decay differs strongly from ^{145g}Gd decay because

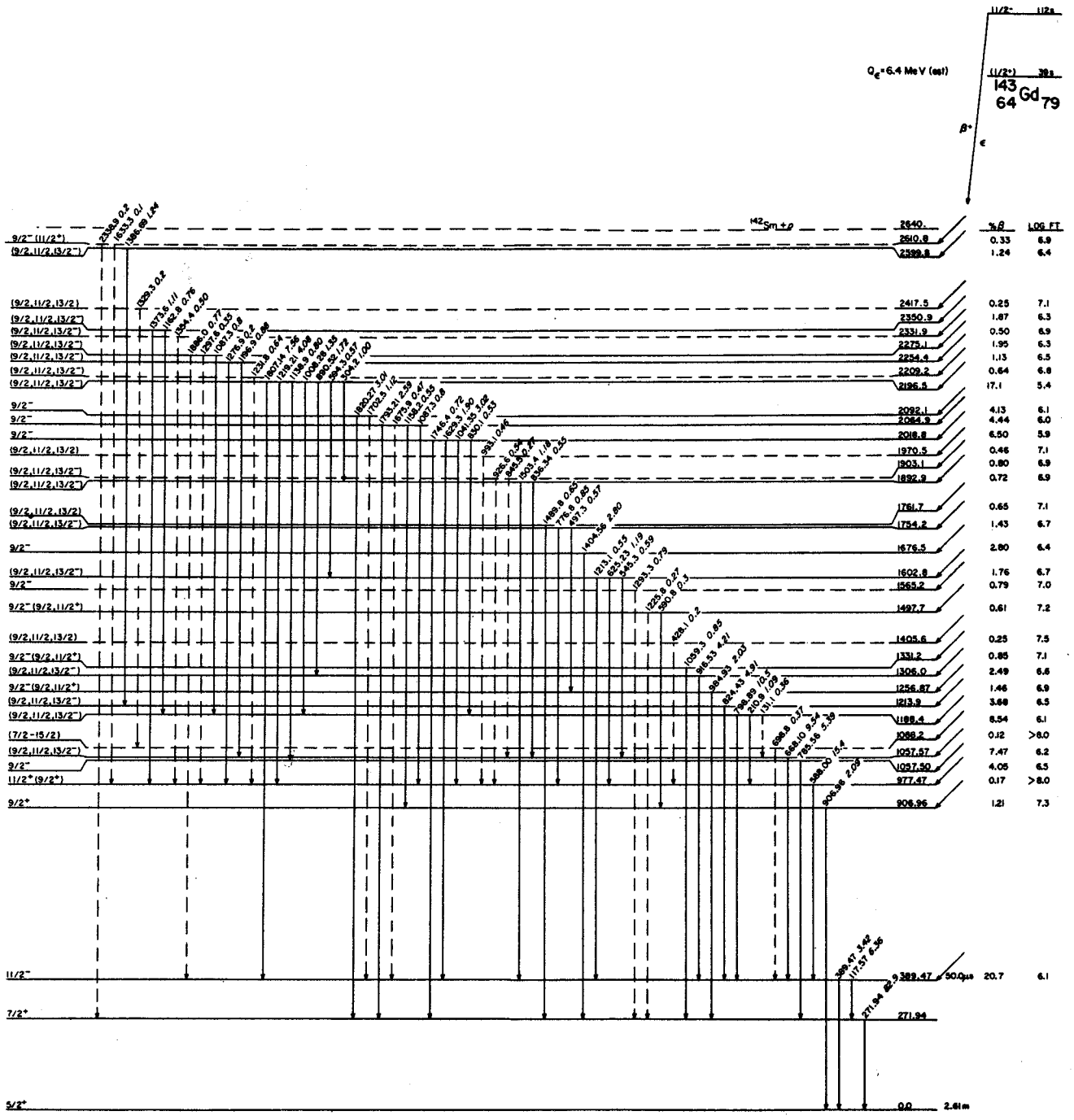

Fig. 3a.--Decay scheme of ^{143m}Gd. $^{143}_{63}Eu_{80}$

of the low log ft values to low-lying states. This is very similar to ^{141g}Sm decay, but differs markedly from all other N=79 decays which exhibit much larger log ft values. We have postulated decay to an unseen low-lying level in ^{143}Eu to explain the apparent log ft values but have not demonstrated this as a fact. If such is the case, then ^{143}Eu must be a deformed nucleus.

We have no evidence as to the excitation energy of the ^{143m}Gd metastable state, but from systematics it is presumed to be small. This is also considered to be the $(\nu h_{11/2})$ $11/2^-$ metastable state which is seen throughout this region. ^{143m}Gd is most notable for its similarity to ^{141m}Sm [R.E. Eppley, R.R. Todd, Wm. C. McHarris, and W.H. Kelly, Phys. Rev. C5, 1084(1972] and ^{139m}Nd decays, which we have previously studied. The decay goes strongly to states at about 2 MeV of excitation which are of complex structure. Presumably these states have large 3-quasiparticle character (cf. the paper on the decay of ^{141m}Sm for a more detailed analysis of this type of state and the paper on the decay of ^{145g}Gd for a similar discussion of the complex states populated by ^{143g}Gd) which offer more open channels for the β^+ decay. It is also notable that no levels are seen above 2640 keV, the proton separation energy. Presumably this is because proton emission competes strongly with γ-rays in this region, although at higher excitations the high level density makes it unlikely to see specific levels. Preliminary studies indicate that a weak proton decay branch of one part in 3×10^5 exists, but we still have only poor statistics of this phenomenon.

In the future we plan to pursue the charged-particle decay work in $^{143g+m}$Gd, as well as look at more neutron-deficient nuclei. Work has already begun on the ^{141}Gd and ^{139}Sm decays. We are also at a good point to consider the theoretical explanations of the N=79 and Z=64 series in terms of explaining the structure of the interesting high-lying levels, and with the help of B.H. Wildenthal we are setting up to do shell-model calculations on these nuclei below N=82.

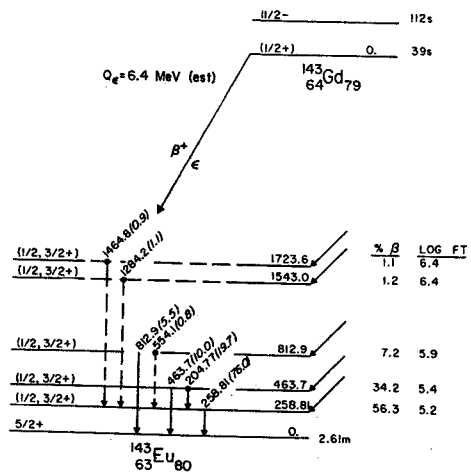

Fig. 3b.--Decay scheme of ^{143g}Gd.

The ε/β^+ Decay of ^{145g}Gd to High Excitation States in ^{145}Eu

R.B. Firestone, R.A. Warner, Wm.C. McHarris, and W.H. Kelly

The decay of ^{145g}Gd has offered a wealth of information about both nuclear states and the weak interaction. An early question raised by ^{145g}Gd was why it decayed so strongly to states at 1758- and 188-keV but not at all to the ground state in complete variance with the lighter off N=81 decays. This question was resolved by suggesting that at ^{145g}Gd the $\nu s_{1/2}$ shell model state crossed the $\nu d_{3/2}$ state to become the ground state. The direct ground state decay was now forbidden, and beta decays through the low lying single particle states were strongly hindered due to very small $\nu s_{1/2}$ or $\nu d_{3/2}$ admixtures in the ^{145g}Gd wavefunction. The most straightforward transitions available were to relatively pure 3-quasiparticle states above the pairing gap in ^{145}Eu which may actually have involved shell model states beyond the N=82 closed shell.

The next interesting question concerned the systematics of the $\nu h_{11/2}$ isomers in the odd N=81 nuclei. Starting at ^{139}Ce the $11/2^-$ states were all at a nearly constant excitation of about 755-keV, and the respective B(M4)'s were virtually constant from ^{135}Xe to ^{143}Sm. For ^{145m}Gd the B(M4) was shown to remain nearly the same, but the M4 transition was now only 721-keV. The absolute excitation was not known because the $\nu d_{3/2} \rightarrow \nu s_{1/2}$ transition was unobserved, but it did not seem reasonable for the absolute excitation to remain constant after the ground state crossing. Nevertheless, an ingenious experiment[2] showed that the $\nu d_{3/2}$ level was at 27-keV placing the $\nu h_{11/2}$ at 749-keV. Indeed, work by Rainis et al[3] has shown that the $\nu h_{11/2}$ in ^{147}Dy is at 752-keV in remarkable constancy with the previous four N=81 nuclei. This result is not easily explained by shell model considerations and suggests a collective phenomenon occuring in supposedly good shell model nuclei.

The next exciting phenomenon for ^{145g}Gd decay involved some rough ε/β^+ decay branching ratio measurements which seemed to deviate widely from normal allowed decay predictions. In our attempts to remove these discrepancies [4,5], we instead verified anomalies of factors as large as 40 for each measureable ^{145g}Gd transition. From this initial work we have branched into a complete reevaluation of ε/β^+ decay theory which has shown that second order affects must be considered in hindered decays. This revelation has brought into question the use of ε/β^+ ratios for determining decay of the weak interaction process.

With so much rewarding information from one nucleus, ^{145}Gd might have been allowed to retire gracefully back to the chart of the nuclides. Nevertheless, to our surprise, ^{145}Gd has snapped back with yet another enigma to be pursued. In the process of cleaning up to last uncertainties in the ^{145g}Gd decay scheme, a spectrum was accumulated concentrating on the higher energy γ-ray transitions. The resulting spectrum is shown in Fig. 1 where, in the region above 3 MeV, over 100 resolvable γ-ray transitions are observed. Although some of these transitions may be escape peaks, it is very likely that most are direct ground state transitions because these decays are generally allowed transitions to spin $1/2^+$ or $3/2^+$ levels which should strongly deexcite to the ground state. These decay systematics are very unusual in that most nuclei are seen to decay only weakly to high lying states which are generally not resolvable. The potential interest in these transitions is multifold because here we may study high lying, low spin states for level density systematics, beta delayed proton decay probabilities, and beta decay rates which reveal information about the tail of the Gamow-Teller giant analogue state in ^{145}Eu. This wealth of new information from ^{145g}Gd may well occupy us for some time to come, but should anyone believe that the end is now in sight it must be pointed out that we have only scratched the surface on ^{145m}Gd decay.

REFERENCES

1. R.E. Eppley, Wm.C. McHarris, and W.H. Kelly, Phys. Rev. C2, 1929(1970).

2. R.B. Firestone, R.A. Warner, Wm.C. McHarris, and W.H. Kelly, Phys. Rev. C11, 1864(1975).

3. A.E. Rainis, K.S. Toth, E. Newman, C.R. Bingham, H.K. Carter, and W.D. Schmidt-Ott, Phys. Rev. C13, 1609(1976).

4. R.B. Firestone, R.A. Warner, Wm.C. McHarris and W.H. Kelly, Phys. Rev. Lett. 33, 30(1974).

5. R.B. Firestone, R.A. Warner, Wm.C. McHarris, and W.H. Kelly, Phys. Rev. Lett. 35, 401(1975).

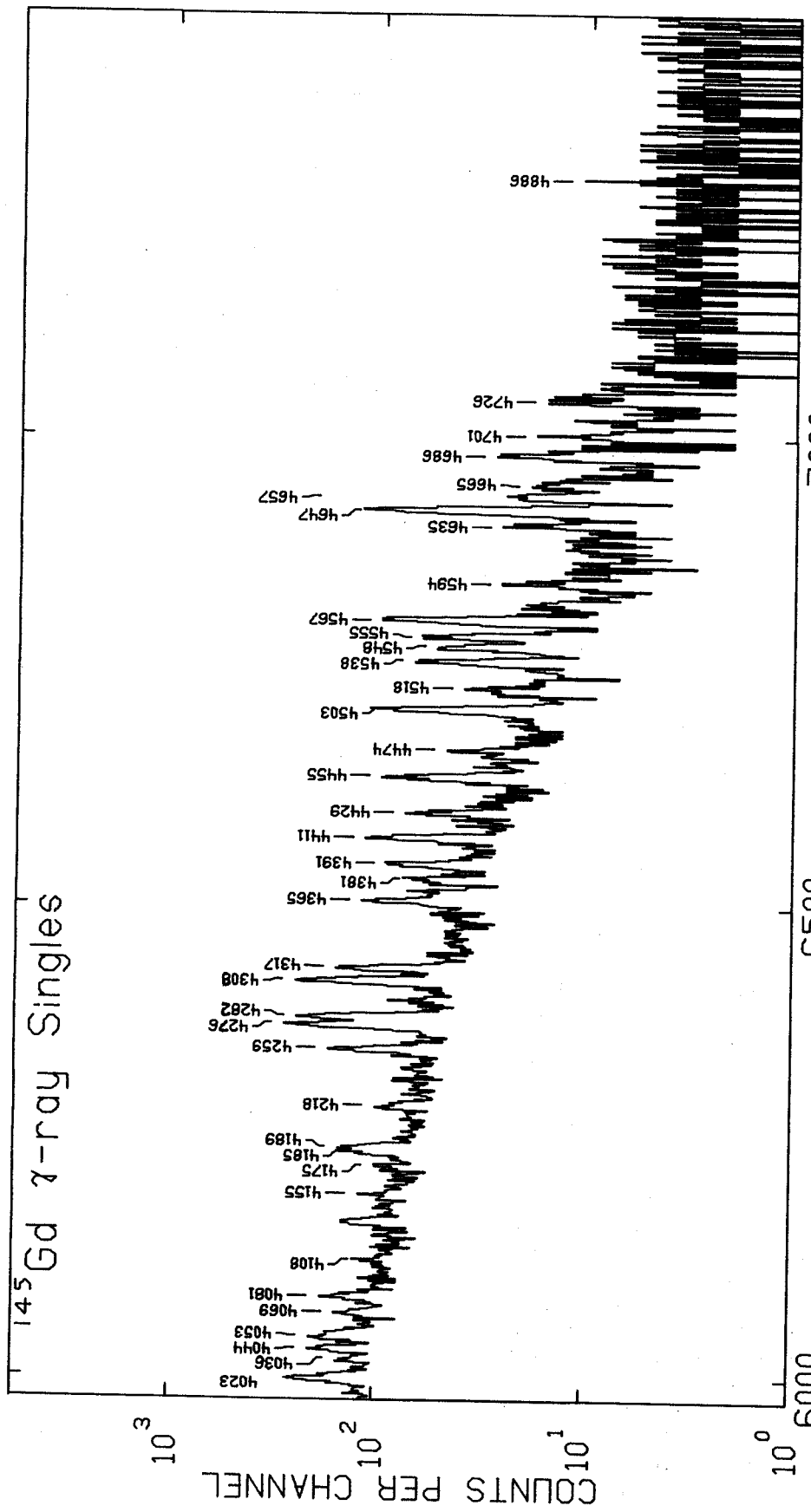

Fig. 1. γ-rays >4 MeV produced following ^{145g}Gd ε/β$^+$ decay.

The ^{22}Na Anomalous ε/β^+ Decay Branching Ratio

R.B. Firestone, B.R. Holstein and Wm. C. McHarris

The ^{22}Na ε/β^+ decay branching ratio is perhaps the best measured such ratio with $(\varepsilon/\beta^+)_{exp}$ = 0.1045(5).[1] This differs from the normal allowed theoretical ratio $(\varepsilon/\beta^+)_{th}$ = 0.1135(3)[1] by 7.9 ± 0.7%. No reasonable explanation has previously been offered for this deviation since exchange and overlap affects were eliminated from consideration.[3] We now believe that second-order terms, ignored in normal allowed calculations, are responsible for this and other ε/β^+ anomalies, as is discussed in another report. It was shown that three important second-order terms would be likely to bring about such anomalies in hindered transitions, and ^{22}Na, with log ft=7.40, may be a primary example. The first term is the weak magnetism $V_{F_{111}}^{(0)}$ matrix element. For ^{22}Na decay it may be possible to observe the analogue M1 γ-ray transition and apply the Conserved Vector Current hypothesis to obtain $V_{F_{111}}^{(0)}$. Currently, only an upper limit is placed on this M1 γ-ray branch, but experiments are in progress to make a more definitive measurement. The sign of $V_{F_{111}}^{(0)}$, relative to the Gamow-Teller matrix element $A_{F_{101}}^{(0)}$, must also be known because, for weak magnetism to account for the observed ε/β^+ ratio, $V_{F_{111}}^{(0)}/A_{F_{111}}^{(0)}$ must have a sign opposite it that of all other known β^+ decays. Recent shell model calculations in this laboratory[4] indicate that indeed $V_{F_{111}}^{(0)}/A_{F_{101}}^{(0)}$ has the desired sign, however, $A_{F_{101}}^{(0)}$ is nearly zero making the calculated sign highly unreliable. Nevertheless, it appears that $V_{F_{111}}^{(0)}$ is dominated by the orbital $\int \alpha x r$ term and may very well have an unusual sign.

The second-class current term, $A_{F_{110}}^{(0)}$, and the $A_{F_{121}}^{(0)}$ term are not so readily elucidated. They are both strongly energy dependent, so therefore it seems possible that well measured beta spectral shapes will help determine them. These measurements are extremely difficult because the affects are small however published measurements indicate non-allowed shapes.[5,6,7] Unfortunately, the existing measurements were not fully analyzed with the current existing theories, and we are now reanalyzing the available data. The β-γ directional correlation has also been measured to give the largest angular correlation coefficient, $A=(1.8\pm0.4)\times 10^{-3}$, of any known allowed transition.[8] This correlation may be useful however it appears that directional correlations depend on tensors of rank 2 as well and may add further complications to the analysis. The energy dependence of the directional correlation or a circular polization of the γ-ray would be most useful in unraveling this problem.

It appears now that the four principle matrix elements, $A_{F_{101}}^{(0)}$, $V_{F_{111}}^{(0)}$, $A_{F_{110}}^{(0)}$, and $A_{F_{121}}^{(0)}$ may be well established by the five experimental numbers ft, ε/β^+, spectral shape factor, M1 γ-ray analogue, and β-γ correlation. If these experiments provide sufficient accuracy, it may be possible to confirm the existence of second class currents and test CVC theory. It is clear that the decay of ^{22}Na offers an excellent opportunity to probe the weak interaction.

REFERENCES

1. J.L. Fitzpatrick, K.W.D. Ledingham, J.Y. Gourlay, and J.G. Lynch, in Proceedings of the International Conference on Inner Shell Ionization Phenomena and Future Applications, Atlanta, Georgia, 1972, edited by R.W. Fink, J.T. Manson, I.M. Palms, and R.V. Rao, CONF-720 404(U.S. Atomic Energy Commission, Oak Ridge, Tenn., (1973), p. 2013.
2. Calculated at the MSU Cyclotron Sigma-7 computer Laboratory with the beta decay code SKEW by R.B. Firestone.
3. A. Williams, Nucl. Phys. A117, 238(1968).
4. W. Chung and B.H. Wildenthal, unpublished.
5. J.H. Hamilton, L.M. Langer, and W.G. Smith, Phys. Rev. 112, 2010(1958).
6. W.H. Brantley, W.B. Newbolt, and J.H. Hamilton, J. Phys. 181, 196 (1964).
7. H. Wenninger, J. Stiewe, and H. Leutz, Nucl. Phys. A109, 561(1968).
8. R.M. Steffen, Phys. Rev. Lett. 3, 277(1959).

The Contribution of Second-Order Processes to ε/β^+ Decay Branching Ratios

R.B. Firestone and B.R. Holstein

ε/β^+ branching ratios have traditionally been calculated using the allowed approximation.[1] This approximation assumes that the lepton wave functions are constant over the nucleus, and that relativistic terms may be neglected. The body of experimental data collected to date indicates only fair agreement with theory, and deviations as large as factors of 40 were reported for ^{145}Gd decay.[2,3] In order to explain these deviations, we suggested that terms through second order in the multipole expansion of the relativistic lepton wave functions must also be included.[4] These terms are normally or order $(qR)^2$, $(v/c)^2$ or $(qR)(v/c)$ and are of magnitude <1% with respect to the large terms for unhindered decays of light nuclei. For heavy nuclei (large R) and hindered decays these terms may contribute more significantly, especially when the normal allowed matrix elements are hindered more than the second-order ones.

Two, essentially equivalent, formalisms have been developed to perform beta decay calculations through second-order. The first formalism is by Behrens and Jänecke[5] and involves a multipole expansion about the nuclear radius with inclusion of the appropriate coulomb, finite size, and screening affects. The important second order matrix elements are called $V_{F_{111}}^{(0)}$, $A_{F_{110}}^{(0)}$, and $A_{F_{121}}^{(0)}$. The second formalism is that of Holstein and Treiman.[6] Here the elementary particle approach is chosen and the expansion is about E/M. The two formalisms are related by the following equations:

$$a = V_{F_{000}}^{(0)}$$

$$b = -\sqrt{3/2}\ V_{F_{111}}^{(0)}$$

$$c = \frac{A_{F_{101}}^{(0)} - W_o R/\sqrt{3}\ A_{F_{110}}^{(0)}}{1 + W_o/2M}$$

$$d = \frac{A_{F_{101}}^{(0)} + 2MR/\sqrt{3}\ A_{F_{110}}^{(0)}}{1 + W_o/2M}$$

$$c_2 = c\,(A_{F_{101}}^{(1)}/A_{F_{101}}^{(0)} - \sqrt{2}/5\ A_{F_{121}}^{(0)}/A_{F_{101}}^{(0)}$$

The b term is essentially the contribution from weak magnetism, and the d term is a second-class current which is non-zero only under G-parity violation. Further discussion in this report will be presented in the Behrens-Jänecke formalism.

The weak magnetism contribution alone gives the following contribution to the ε/β^+ ratio

$$(\varepsilon/\beta^+)_{w.m.} = (\varepsilon/\beta^+)_{allowed}\,[1+4\sqrt{2/3}\sqrt{3}\ (W_k+\bar{W})R \times V_{F_{111}}^{(0)}/A_{F_{101}}^{(0)}].$$

Clearly the absolute size of the weak magnetism term is less important than its size relative to $A_{F_{101}}^{(0)}$. For very hindered decays, $V_{F_{111}}^{(0)}$ may have a profound effect on the ε/β^+ decay branching ratio. The affect of the second-class current is essentially seen by $A_{F_{110}}^{(0)}$ where

$$(\varepsilon/\beta^+)_{s.c.c.} = (\varepsilon/\beta^+)_{allowed}\,[1+1/2\sqrt{1/3}\ \alpha \times A_{F_{110}}^{(0)}/A_{F_{101}}^{(0)}].$$

If $A_{F_{110}}^{(0)}$ is sufficiently less hindered than $A_{F_{101}}^{(0)}$, it is possible to observe a large contribution by the second-class current to the ε/β^+ decay branching ratio. Finally, there is a correction from $A_{F_{121}}^{(0)}$ of the form

$$(\varepsilon/\beta^+)_{121} = (\varepsilon/\beta^+)_{allowed}\,\{1+2/3\sqrt{2}\ A_{F_{121}}^{(0)}/A_{F_{101}}^{(0)}\ [(\bar{W}+W_x)\ (W_o-\bar{W}+W_x+3\alpha Z/2R)(R^2/9)]\}$$

As in the previous terms, $A_{F_{121}}^{(0)}$ can also contribute to the ε/β^+ decay branching ratio for very hindered transitions.

These three terms are probably the main contributions to the apparent anomalies which exist in the literature for measured ε/β^+ decay branching ratios. The equations presented are approximate, and one should rigorously follow the full treatment, according to Behrens-Jänecke, for the best calculation.

REFERENCES

1. E.g. N. Gove and M.J. Martin, Nucl. Data, Sect. A 10, 205(1971).
2. R.B. Firestone, R.A. Warner, Wm.C. McHarris, and W.H. Kelly, Phys. Rev. Lett. 33,30(1974).
3. R.B. Firestone, R.A. Warner, Wm.C. McHarris, and W.H. Kelly, Phys. Rev. Lett. 35,401(1975).
4. R.B. Firestone, R.A. Warner, Wm.C. McHarris, and W.H. Kelly, Phys. Rev. Lett. 35, 713(1975).
5. H. Behrens and J. Jänecke, Numerical Tables for Beta-Decay and Electorn Capture, edited by H. Schopper, in Landolt-Börnstein Numerical Data and Functional Relationships in Science and Technology, edited by K.H. Hellwege (Springer, Berlin, 1969), Group I, Vol. 4.
6. "The ^{22}Na Anomalous ε/β^+ Decay Branching Ratio" report.

A Compilation of Experimental ε/β^+ Decay Branching Ratios

R.B. Firestone

As an off-shoot of our ε/β^+ decay branching ratio measurements in the rare earth region, we have performed a literature search for other experimental values. The measurements we did on ^{145}Gd[1,2] indicated deviations from normal allowed calculations by factors as large as 40. It was of some concern to us as to whether our measurements were the only deviations from theory, or whether other anomalies might exist. It now seems well understood that the normal allowed calculations, traditionally performed, are not precise because they neglect such features as weak magnetism, second class currents, and other second order affects which may contribute by several percent even to superallowed transitions.[3] When severely hindered transitions are considered, the second order affects may actually dominate the decay branching ratios possible for such decays. It is therefore important that ε/β^+ decay branching ratios be studied in order to understand the second order affects which may contain fundamental insights into the weak interaction.

Although a thorough search of the literature is unfeasible for unearthing all of the measured ε/β^+ decay branching ratios, numerous authors have provided tabulations of measured ε/β^+ ratios.[4,5,6,7,8] These tend to be rather incomplete lists, but not all authors overlap allowing a more complete list to be distilled from all sources. In addition, a large number of the ε/β^+ measurements lie buried in the Nuclear Data Sheets.[9] A thorough search through all compiled A chains has uncovered many new ε/β^+ ratios measurements. Unfortunatly, not all of the compilers reported measured ε/β^+ ratios and so it is certain that gaps exist in this compilation. In Table I we included 71 ε/β^+ ratios for allowed transitions, and 20 ε/β^+ ratios for forbidden transitions. The calculated values in Table I are those of Gove and Martin.[10] In addition, a skew ratio $\forall$ is defined as the ratio of experiment to theory.

It is evident that many of the tabulated ε/β^+ ratios differ significantly from theory. This seems particularly true when the best measured values such as ^{22}Na are considered. The error bars on the theory reflect uncertainty in the decay energies, and better mass measurements will significantly improve many of the values. It appears that the ^{145}Gd measurements are indeed more anomalous than the others. This is not so surprising if one considers that these are unusually hindered transitions from a higher Z nucleus. Most good measurements were done for fast decays in lower Z nuclei where strong theoretical limits exist on the extent of an anomaly. As Z increases and the transitions become more hindered, we see a general increase in the extent of the anomalies. As a rule only first forbidden unique transitions have been considered calculable among the forbidden decays. Here only moderate agreement with theory is found.

REFERENCES

1. R.B. Firestone, R.A. Warner, Wm.C. McHarris, and W.H. Kelly, Phys. Rev. Lett. 33, 30(1974).
2. R.B. Firestone, R.A. Warner, Wm.C. McHarris, and W.H. Kelly, Phys. Rev. Lett. 35, 401(1975).
3. R.B. Firestone and B. Holstein, unpublished.
4. D. Berenyi, Nucl. Phys. 48, 121(1963).
5. H.F. Schopper, Weak Interactions and Nuclear Beta Decay, North Holland Publishing Co., Amsterdam, 1966.
6. E.J. Konopinski, The Theory of Beta Radioactivity, Clarendon Press, Oxford, 1966.
7. E.I. Biryukob and N.S. Shimanskaya, Yad. Fiz. 11, 246(1970).
8. M.L. Fitzpatrick, K.W.D. Ledingham, J.Y. Gourlay, and J.G. Lynch, in Proceedings of the International Conference on Inner Shell Ionization Phenomena and Future Applications, Atlanta, Georgia, 1972 edited by R.W. Fink, J.T. Manson, I.M. Palms, and R.V. Rao, CONF-720 404(U.S. Atomic Energy Commission, Oak Ridge, Tenn., (1973), p. 2013.
9. Nuclear Data Sheets, Volumes 1-1 through 18-4.
10. N.B. Gove and M.J. Martin, Nucl. Data Tables 10, 205(1971).

Table I Measured and Calculated ε/β^+ Decay Branching Ratios

Transition	Log ft	Q_{β^+}(MeV)	ε/β^+ Experiment	ε/β^+ Theory	(exp/theory)
$^{11}_{6}C(3/2^-\rightarrow 3/2^-)$	3.59	0.9602	$(2.30\pm0.13)\times10^{-3}$ [a]	$(2.316\pm0.010)\times10^{-3}$	0.99 ± 0.06
$^{13}_{7}N(1/2^-\rightarrow 1/2^-)$	3.66	1.1995	$(1.68\pm0.12)\times10^{-3}$ [a]	$(1.939\pm0.006)\times10^{-3}$	0.87 ± 0.06
$^{15}_{8}O(1/2^-\rightarrow 1/2^-)$	3.64	1.7372	$(1.07\pm0.06)\times10^{-3}$ [a]	$(0.969\pm0.002)\times10^{-3}$	1.10 ± 0.06
$^{18}_{9}F(1^+ \rightarrow 0^+)$	3.55	0.6333	$(3.00\pm0.18)\times10^{-2}$ [a]	$(3.31\pm0.02)\times10^{-2}$	0.91 ± 0.06
$^{19}_{10}Ne(1/2^+\rightarrow 1/2^+)$	3.23	2.2162	$(9.6\pm0.3)\times10^{-4}$ [a]	$(9.75\pm0.02)\times10^{-4}$	0.98 ± 0.03
$^{22}_{11}Na(3^+ \rightarrow 2^+)$	7.40	0.5457	0.1045 ± 0.0005	0.1130 ± 0.0004	0.925 ± 0.008
$^{30}_{15}P(1^+ \rightarrow 0^+)$	4.84	3.205	$(1.24\pm0.04)\times10^{-3}$ [a]	$(1.260\pm0.004)\times10^{-3}$	0.98 ± 0.03
$_{21}Sc(2^+\rightarrow 2^+)$	5.30	1.481	0.073 ± 0.016 0.023 ± 0.019	0.0487 ± 0.0004	
$^{48}_{23}V(2^+\rightarrow 2^+)$	6.2	0.698	0.77 ± 0.03	0.767 ± 0.012	1.00 ± 0.06
$^{52}_{25}Mn(6^+\rightarrow 6^+)$	5.6	0.575	1.92 ± 0.07	2.09 ± 0.03	0.92 ± 0.05
$^{52}_{26}Fe(0^+\rightarrow 1^+)$	4.7	0.80	0.64 ± 0.05	0.78 ± 0.03	0.82 ± 0.10
$^{58}_{27}Co(2^+\rightarrow 2^+)$	6.6	0.476	5.82 ± 0.10	5.60 ± 0.13	1.04 ± 0.04
$^{57}_{28}Ni(3/2^-\rightarrow 3/2^-)_1$	5.6	0.851	0.81 ± 0.04	0.88 ± 0.02	0.92 ± 0.07
$(3/2^-\rightarrow 3/2^-)_2$	6.1	0.471	6 ± 1	6.7 ± 0.4	0.9 ± 0.2
$(3/2^-\rightarrow 1/2^-)_1$	6.1	0.723	1.44 ± 0.06	1.53 ± 0.05	0.94 ± 0.07
$(3/2^-\rightarrow 1/2^-)_2$	5.6	0.309	27 ± 3	32 ± 3	0.84 ± 0.17
$^{61}_{29}Cu(3/2^-\rightarrow 3/2^-)$	5.1	1.223	0.24 ± 0.04	0.312 ± 0.002	0.77 ± 0.13
$^{64}_{29}Cu(1^+\rightarrow 0^+)$	4.9	0.655	2.2 ± 0.2	2.56 ± 0.03	0.86 ± 0.11
$^{65}_{30}Zn(5/2^-\rightarrow 3/2^-)$	7.46	0.329	30.1 ± 0.7	34.4 ± 0.5	0.88 ± 0.03
$^{68}_{31}Ga(1^+\rightarrow 0^+)$	5.2	1.899	0.11 ± 0.02	0.1025 ± 0.0002	1.08 ± 0.20
$(1^+\rightarrow 2^+)$	5.5	0.822	1.42 ± 0.13	1.502 ± 0.008	0.95 ± 0.09
$^{77}_{35}Br(3/2^-\rightarrow 1/2^-)$	5.7	0.342	45 ± 11	60.3 ± 2.1	0.75 ± 0.21
$^{79}_{36}Kr(1/2^-\rightarrow 3/2^-)_1$	6.1	0.343	64 ± 11	68 ± 5	0.94 ± 0.22
$(1/2^-\rightarrow 3/2^-)_2$	6.1	0.306	480 ± 112	520 ± 65	0.9 ± 0.3
$^{87}_{39}Y(1/2^-\rightarrow 1/2^-)$	6.7	0.472	55 ± 7	29.8 ± 1.5	1.9 ± 0.3
$(9/2^+\rightarrow 9/2^+)$	7.5	$^{1.24}_{1.15}$	1.04 ± 0.16	1.04 ± 0.02 1.34 ± 0.16	1.00 ± 0.17 0.78 ± 0.21
$^{89}_{40}Zr(9/2^+\rightarrow 9/2^+)$	6.15	0.900	3.44 ± 0.04	3.39 ± 0.04	1.01 ± 0.03
$(1/2^-\rightarrow 3/2^-)$	4.30	0.890	3.76 ± 0.19	3.51 ± 0.04	1.07 ± 0.07
$^{92}_{41}Nb(2^+\rightarrow 2^+)$	6.2	0.19	1680 ± 170	1514 ± 350	1.1 ± 0.4
$^{104}_{48}Cd(0^+\rightarrow 1^+)$	4.2	0.2	95 ± 30	>575	<0.17
$^{107}_{48}Cd(5/2^+\rightarrow 7/2^+)$	5.0	0.302	361 ± 23	488 ± 27	0.74 ± 0.09
$^{111}_{50}Sn(7/2^+\rightarrow 9/2^+)$	4.8	1.49	2.30 ± 0.12	1.76 ± 0.10	1.31 ± 0.15
$^{115}_{51}Sb(5/2^+\rightarrow 3/2^+)$	4.7	1.51	1.22 ± 0.06	1.87 ± 0.08	0.65 ± 0.06
$^{116}_{51}Sb(8^-\rightarrow 7^+)$	4.8	1.17	4.21 ± 0.17	4.36 ± 0.52	0.97 ± 0.16
$^{118}_{51}Sb(8^-\rightarrow 7^-)$	5.0	0.31	625 ± 39	617 ± 120	1.0 ± 0.2
$^{120}_{51}Sb(1+\rightarrow 0^+)$	4.51	1.659	1.207 ± 0.040	1.39 ± 0.02	0.87 ± 0.04
$^{121}_{53}I(5/2^+\rightarrow 3/2^+)$	5.2	1.14	6.3 ± 0.9	5.7 ± 0.7	1.1 ± 0.3
$^{128}_{53}I(1^+\rightarrow 0^+)$	5.1	0.232	2070 ± 460	2655 ± 196	0.78 ± 0.23
$^{120}_{54}Xe(0^+\rightarrow 1^+)$	4.97	0.9	14.3 ± 2.0	$14\pm^{24}_{7}$	>0.37
$^{123}_{55}Cs(1/2^+\rightarrow 3/2^+)$	5.6	2.6	0.581 ± 0.006	0.5 ± 0.3	>0.75
$^{134}_{57}La(1^+\rightarrow 0^+)$	4.9	2.67	0.50 ± 0.03	0.552 ± 0.016	0.91 ± 0.08

Transition	Log ft	Q_β(MeV)	ε/β^+		
			Experiment	Theory	(exp/theory)
$^{187}_{59}Pr(5/2^+ \rightarrow 3/2^+)$	5.4	1.684	2.74±0.34	2.72±0.05	1.01±0.14
$^{138}_{59}Pr(8^- \rightarrow 7^-)$	5.6	1.29	5.2±1.4	6.58±0.18	0.79±0.23
$^{139}_{59}Pr(5/2^+ \rightarrow 3/2^+)$	5.6	1.09	13.1±1.2	11.6±0.8	1.13±0.18
$^{140}_{59}Pr(1^+ \rightarrow 0^+)$	4.4	2.366	0.86±0.03	0.948±0.007	0.91±0.04
$^{136}_{60}Nd(0^+ \rightarrow 1^+)$	6.3	1.29	15.2±0.6	7.1±0.9	2.1±0.3
$^{139}_{60}Nd(3/2^+ \rightarrow 5/2^+)$	5.1	1.76	2.4±0.2	2.59±0.24	0.93±0.17
$^{141}_{60}Nd(3/2^+ \rightarrow 5/2^+)$	5.2	0.78	33.5±2.1	40.6±2.3	0.83±0.10
$^{143}_{62}Sm(3/2^+ \rightarrow 5/2^+)$	4.94	2.46	1.11±0.05 1.48±0.13	1.09±0.05	1.02±0.09 1.36±0.18
$^{145}_{64}Gd(1/2^+ \rightarrow 1/2^+)_1$	7.3	3.5	18±8	0.45±0.05	40±22
$(1/2^+ \rightarrow 3/2^+)_1$	6.7	3.2	0.84±0.05	0.56±0.07	1.50±0.27
$(1/2^+ \rightarrow 1567)$	7.5	2.7	36±18	0.95±0.13	38±25
$(1/2^+ \rightarrow 1599)$	7.2	2.7	12±6	0.99±0.14	12±8
$(1/2^+ \rightarrow 3/2^+)_2$	5.8	2.5	1.97±0.09	1.19±0.17	1.66±0.30
$(1/2^+ \rightarrow 1762)$	7.2	2.5	2.5±0.8	1.19±0.18	2.1±1.0
$(1/2^+ \rightarrow 1845)$	7.6	2.4	43±21	1.31±0.20	33±21
$(1/2^+ \rightarrow 3/2^+)_3$	5.8	2.4	2.41±0.12	1.37±0.21	1.76±0.36
$(1/2^+ \rightarrow 2049)$	7.1	2.2	4±1	1.72±0.28	2.3±1.0
$(1/2^+ \rightarrow 2114)$	7.6	2.2	10±4	1.88±0.33	5.3±3.0
$(1/2^+ \rightarrow 2495)$	6.9	1.8	4.8±0.5	3.42±0.72	1.4±0.5
$(1/2^+ \rightarrow 2642)$	6.7	1.6	8.2±0.9	4.48±1.05	1.8±0.7
$^{155}_{66}Dy(3/2^- \rightarrow 5/2^-)$	6.3	0.850	39±10	50.1±1.4	0.78±0.22
$^{166}_{71}Lu(6^- \rightarrow 7^-)$	4.7	2.2	3.04±0.25	3.05±0.70	1.00±0.31
$^{178}_{73}Ta(1^+ \rightarrow 0^+)$	4.7	0.89	87±12	75.5±2.7	1.15±0.20
$(1^+ \rightarrow 2^+)$	4.9	0.80	113±22	112±5	1.01±0.24
$^{178}_{75}Re(3^+ \rightarrow 4^+)$	6.2	3.3	4.3±1.6	1.28±0.20	3.4±1.8
$(3^+ \rightarrow 2^+)$	6.5	3.5	5.5±1.0	1.06±0.17	5.2±1.8
$^{205}_{83}Bi(9/2^- \rightarrow 7/2^-)$	8.97	0.980	267±76	114±4	2.3±0.7
$(9/2^- \rightarrow 9/2^-)$	9.42	0.696	612±306	407±19	1.5±0.8
$^{205}_{84}Po(5/2^- \rightarrow 7/2^-)_1$	6.63	0.89	190±46	171±8	1.1±0.3
$(5/2^- \rightarrow 7/2^-)_2$	7.5	1.14	69±39	72.1±2.6	1.0±0.6
First Forbidden					
$^{74}_{33}As(2^- \rightarrow 2^+)$	6.96	0.944	1.288±0.018		
$^{84}_{37}Rb(2^- \rightarrow 2^+)$	7.1	0.776	5.7±0.4		
$^{100}_{45}Rh(1^- \rightarrow 0^+)$	8.3	1.49	1.2		
$^{124}_{53}I(2^- \rightarrow 2^+)$	7.5	1.54	3.0		
$^{126}_{53}I(2^- \rightarrow 2^+)$	7.5	0.463	168±5		
$^{132}Cs(2^- \rightarrow 2^+)$	6.7	0.41	62±10		
$^{145}_{63}Eu(5/2^+ \rightarrow 3/2^-)$	7.4	0.80	100±18		
$(5/2^+ \rightarrow 7/2^-)$	8.8	1.70	3.5±0.6		
$^{147}_{63}Eu(5/2^+ \rightarrow 3/2^-)$	8.3	0.443	188±35		
$(5/2^+ \rightarrow 5/2^-)$	8.5	0.519	199±35		
$(5/2^+ \rightarrow 7/2^-)$	8.7	0.740	102±53		
$^{161}_{68}Er(3/2^- \rightarrow 1/2^+)$	6.6	0.82	470±235		
$^{183}_{26}Os(9/2^+ \rightarrow 9/2^-)$	6.56	2.4	690±310		
$^{200}_{81}Tl(2^- \rightarrow 2^+)$	7.3	1.064	129±9		

First Forbidden Unique					
$^{84}_{37}Rb(2^- \rightarrow 0^+)$	8.4	1.658	2.3±0.4	0.837±0.004	2.8±0.5
$^{122}_{51}Sb(2^- \rightarrow 0^+)$	7.9	0.588	300±50	286±4	1.05±0.19
$^{126}_{53}I(2^- \rightarrow 0^+)$	9.0	1.129	23±2	23.5±0.2	0.98±0.09
Second Forbidden					
$^{36}_{17}Cl(2^+ \rightarrow 0^+)$	13.58	0.122	1150±360		
$^{207}_{83}Bi(9/2^- \rightarrow 5/2^-)$	12.6	0.813	600±100		
Second Forbidden Unique					
$^{26}_{13}Al(5^+ \rightarrow 2^+)$	14.18	1.1740	0.19±0.04		

a) K/β^+ measurements

In-Beam Conversion Electron Measurements of the 1099 keV E1 Transition in ^{48}V

W.H. Bentley, F.M. Bernthal, W.H. Kelly, L.L. Kneisel[+], Wm.C. McHarris, L.E. Samuelson[*] and R.A. Warner

Experiments have been performed on ^{48}V to confirm the existence of an earlier reported odd parity rotational band built on a proposed $J^{\pi}=4^{-}$ state at 1099.1 keV[1]. Since then, other experiments have led to a $J^{\pi}=5^{+}$ assignment for this state[2]. Due to the conflicting J^{π} assignments for this level, an unambiguous measurement to resolve the conflicting assignments became necessary. We, therefore, have measured the K internal conversion coefficient for the 1099 keV transition that depopulates this state to the 4^{+} ground state. This measurement makes possible a definite parity assignment for the 1099 keV state.

6.4 MeV protons from the MSU Cyclotron were used to study the $(p,ne^{-}\gamma)$ reaction with a 1 mg/cm^2 metallic ^{48}Ti target (enriched to 99%). The on-line electron spectrometer[3], consisting of a short solenoidal magnet with anti-positron vanes and a Si(Li) detector, was used. The Si(Li) detector is used for energy determination, while the purpose of the magnet is to enhance counting rates, provide gross momentum selection and remove unwanted signals from x-rays and low energy gamma rays. The axis of the spectrometer was oriented at 90°with respect to the beam direction. A Ge(Li) detector oriented at 90°on the other side was used to take the gamma-ray data simultaneously.

Two different modes of operation were used. In the first, data were taken with the spectrometer magnet at a fixed current selected to maximize the detection efficiency for the K electrons from the 1099-keV transition. In the second mode, the magnet was swept at a constant rate over a large energy range. Using the theoretical conversion coefficients of Pauli[4], the K-electron lines from the pure E2 transitions at 983.3 and 1311.7 keV were used as the fiducial lines. These are from the $2^{+}\rightarrow 0^{+}$ and $4^{+}\rightarrow 2^{+}$ transitions in ^{48}Ti that are excited primarily by the (p,p') reaction. Fig. 1 shows the electron spectrum taken in the fixed current mode of operation.

The results of these two experiments are consistent with each other giving values of $4.1\pm 0.6 \times 10^{-5}$ and $3.8\pm 1.0 \times 10^{-5}$, respectively, for the K conversion coefficient. These numbers are clearly in agreement with the theoretical value 4.5×10^{-5} for a pure E1 and not in agreement with either an M1 or an E2 assignment ($\alpha = 8.0 \times 10^{-5}$ and $\alpha = 9.9 \times 10^{-5}$ respectively)[4]. From this result, a definite assignment of

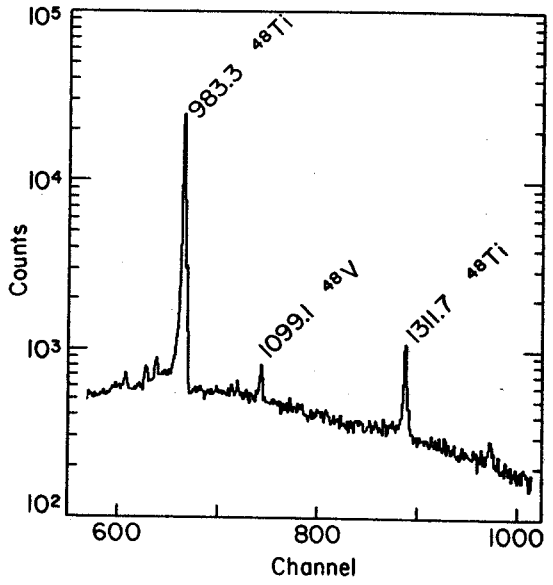

Fig. 1 Internal conversion electron spectrum of the $^{48}Ti(p,ne^{-})^{48}V$ reaction in the region of 809 keV to 1506 keV. Labels give corresponding transition energies.

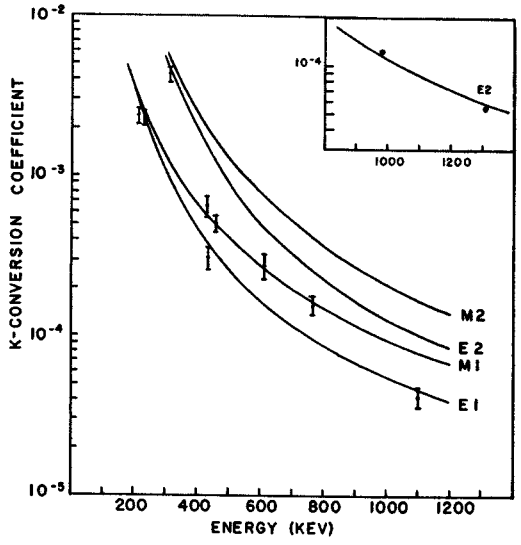

Fig. 2 Internal conversion coefficients for transitions in ^{48}V. Inset shows fiducial lines from ^{48}Ti.

negative parity can be made to the 1099 keV state. In addition, while running in the first mode several other ^{48}V transitions were measured giving K-conversion coefficients consistent with previously accepted spin and parity assignments. Fig. 2 compares the measured conversion coefficients and the theoretical values.

With the spin and parity of the 1099 keV state determined, the existence of a $K^{\pi}=4^-$ rotational band built on this level is confirmed. The resulting decay scheme is shown in Fig. 3. States in the band have been identified up to the 8^- state. This band follows quite well the I(I + 1) rule. Another odd-parity rotation-like band built on the $J^{\pi}=1^-$ state at 519 keV has been previously reported[5]. As can be seen from Fig. 4, the 1^- band is strongly perturbed. These bands can be interpreted as the singlet and triplet couplings of the $\Omega^{\pi}[N\ n_z\Lambda\ \Sigma]=3/2^+\ [202\uparrow]$ proton and $5/2^-\ [312\uparrow]$ neutron Nilsson orbitals. This is a clear indication of permanent prolate deformation at low energies in a nucleus close to Z= N=20 closed shells.

REFERENCES

1. MSUCL Annual Report, 1973-74, p. 53.
2. P. Taras, B. Haas and R. Vaillancourt, Nucl. Phys. A232, 99 (1974).
3. Lawrence L. Kneisel, M.S. Thesis, Michigan State University, 1975; and this report p.
4. H.C. Pauli and U. Raff, Computor Physics Comm. 9, 392 (1975).
5. B. Haas and P. Taras, Phys. Rev. Letters 33, 105(1974).

† Present address: National Semiconductor, Sunnyvale, California

* Present address: Department of Physics, Purdue University, Lafayette, Indiana 47907

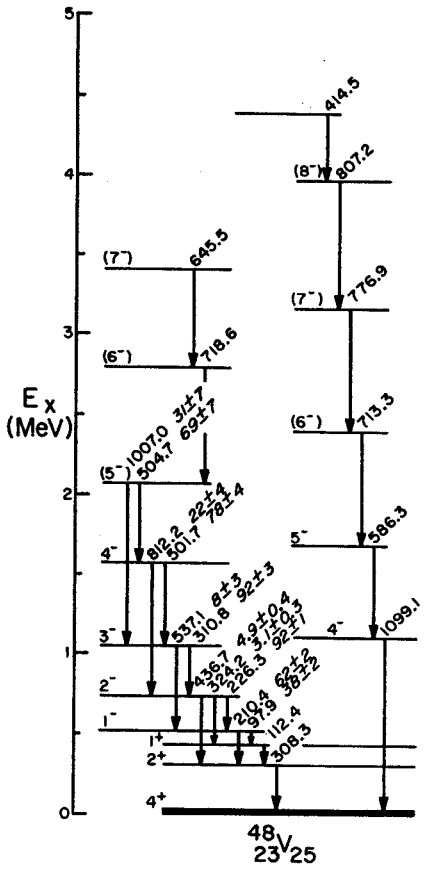

Fig. 3 Negative parity bands in ^{48}V.

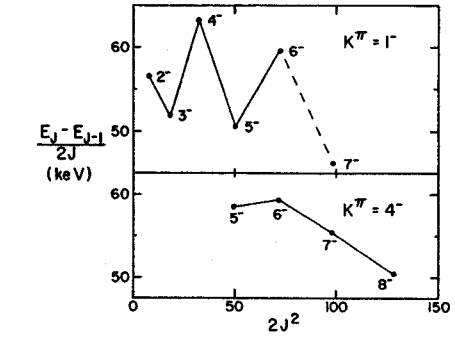

Fig. 4 "Trumpet Plots" for the 1^- and 4^- rotation-like bands in ^{48}V.

β-Recoil Energy Distributions with SIEGFRIED

M.D. Edmiston, R.A. Warner, and Wm. C. McHarris

SIEGFRIED, the MSU on-line mass identification system, has been in routine use for about one year.[1,5] During this period it has come to our attention that the β source, produced in SIEGFRIED by the He-jet, appears to be sufficiently thin to permit many of the β-recoiling nuclei to leave the source with a large percentage of their initial recoil energy. In terms of measuring masses, this is a slight hindrance because it represents an uncertainty in the mass of about 1% for the flight path and accelerating voltage we use. However, it shows promise of being a great asset because it may enable one to measure the energy distributions of the recoils.

Since the time-of-flight (TOF) is proportional to the square-root of the energy, one would expect that the peak shapes in the TOF spectrum would be similar to the β-recoil-energy distribution. This is not quite true since these TOF peaks (i.e., mass peaks) are perturbed by a geometry factor which is dependent on the recoil energy of the recoiling atom. In short, SIEGFRIED's efficiency falls off with increasing recoil energy. This results in a mass peak which is relatively narrow except for a rather long tail on the low-mass side. For example, see ^{26}Al and ^{27}Si in Fig. 1.

Since Fermi and Gamow-Teller decays have different recoil-energy distributions, one would expect the mass peaks resulting from Fermi decays to have slightly different shapes than those resulting from Gamow-Teller decays. Figure 2 shows the calculated distributions for the two types of decay, and leads one to conclude that Gamow-Teller decays should have smaller tails on the mass peaks.[6]

Figure 1 shows a set of data that was taken to test this hypothesis. The ^{26}Al decay is a 0^+ to 0^+ transition and thus pure Fermi. The ^{18}F decay is a 1^+ to 0^+ transition and thus pure Gamow-Teller. The ^{18}F was made by the ^{20}Ne(p,^{3}He)^{18}F reaction and the ^{26}Al was made by the ^{27}Al(p,pn)^{26}Al reaction. Both targets were used in the He-jet simultaneously. The qualitative difference in mass-peak shape is obvious, and is indeed more than we expected. In addition, the ^{29}P peak is without a tail, which may mean that this $1/2^+$ to $1/2^+$ transition is more Gamow-Teller than expected.

It is presently difficult to explain why the shape difference is as great as it is, so further experiments and calculations are underway to help us understand what we see and what its utility will be.

REFERENCES

1. MSU Cyclotron Annual Report 1973-74, p. 86.
2. M. Edmiston, K. Kosanke, Wm. C. McHarris, R.A. Warner, and W.H. Kelly, Bull. Am. Phys. Soc. 20,603(1975).
3. M.D. Edmiston, R.A. Warner, and Wm. C. McHarris, Bull. Am. Phys. Soc. 21,557(1976).
4. M.D. Edmiston, R.A. Warner, Wm. C. McHarris, and W.H. Kelly, in Proceedings of the 3rd International Conference on Nuclei Far From Stability, CERN, 1976; also to be published.
5. M.D. Edmiston, Ph.D. Thesis, Michigan State University, MSUNC-186, 1976.
6. C.S. Wu, and S.A. Moszkowski, Beta Decay, New York: John Wiley and Sons, 1966, p. 111.

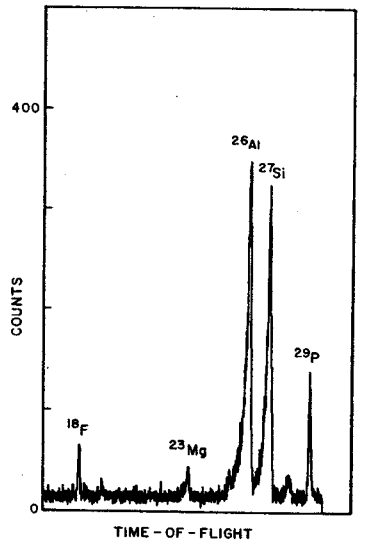

Fig. 1.--"Mass spectrum from SIEGFRIED".

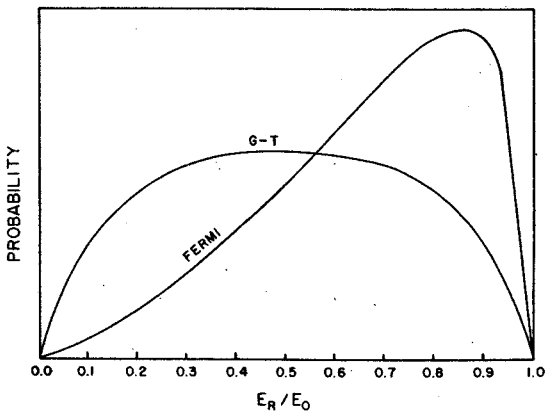

Fig. 2.--"Calculated β-recoil energy distributions."

On-Line ^{46}Ti $(\tau,2n\gamma)$ ^{47}Cr Gamma Ray Studies

R.B. Firestone, R.A. Warner, D. Mueller, and Wm.C. McHarris

^{47}Cr is one of a series of heavy mirror nuclei whose mass has been measured in this laboratory.[1] In addition, ^{47}Cr represents the heaviest mirror nucleus whose half-life has been accurately studied.[2] Mirror nuclei offer a great deal of information about both nuclear structure and the weak interaction. Mirror pairs will differ only through the coulomb force, and therefore the comparison of the masses of the various mirror states will allow us to infer the nature of the charge distribution within the nucleus. The beta decays of the mirror nuclei also represent superallowed transitions which are most tractable for shell model calculations of the Gamow-Teller part of the matrix element. In addition, the apparent vanishing of the Cabibbo angle for ^{35}Ar decay[3] makes it most interesting to look in the heavier mirrors for a similar type effect.

The ground state mass of ^{47}Cr was observed by the $^{50}Cr(^{3}He, ^{6}He)^{47}Cr$ reaction. Numerous excited states were also seen in this reaction, and although the ground state and a 102-keV first excited state were seen only weakly in this reaction, much better statistics were obtained for excited states reported at 182- and 478-keV. The ground state mass could be improved significantly if the γ-ray transitions deexciting those better known states were observed with a high resolution Ge(Li) spectrometer. A series of in-beam γ-ray spectra were taken for 18-, 22-, and 26-MeV ^{3}He beams on a ^{46}Ti target. The primary γ rays observed in these spectra were from the ^{46}Ti $(^{3}He, pn)^{47}V$ reaction. Weak transitions were also observed at 75.2-, 99.3-, and 175.4-keV which were similar to the energies expected for γ rays deexciting the first two excited states of ^{47}Cr. In order to more firmly place these transitions, the measured excitation function was compared with theory by the aid of the particle evaporation code ALICE.[4] Each spectrum was normalized with respect to the strong 88-keV transition in ^{47}V. Although the statistics were poor for the transitions of interest, in Fig. 1 we show that they agree statisfactorily with the expected excitation function for ^{47}Cr. Only the $^{46}Ti(^{3}He, ^{4}He p\gamma)^{44}Sc$ reaction gives a similar excitation curve, andnone of the transitions of interest are previously observed in ^{44}Sc.

We therefore suggest the tentative level scheme in Fig. 2 with the first excited state at 99.3 ± 0.5 keV and the second state at 175 ± 1 keV in part on the basis of the agreement with the ^{3}He, ^{6}He) work, although the observed transitions may be from ^{44}Sc or ^{44}Ti. Further work is planned to obtain better γ-ray energy calibrations and run different excitation energies in order to confirm the placements of these transitions.

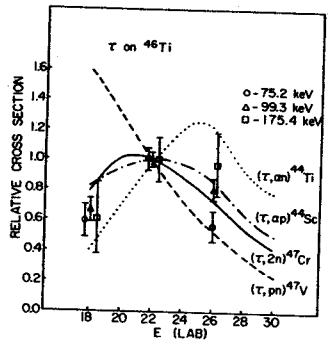

Fig. 1 Comparison of experimental and theoretical relative cross sections for the proposed ^{47}Cr transitions.

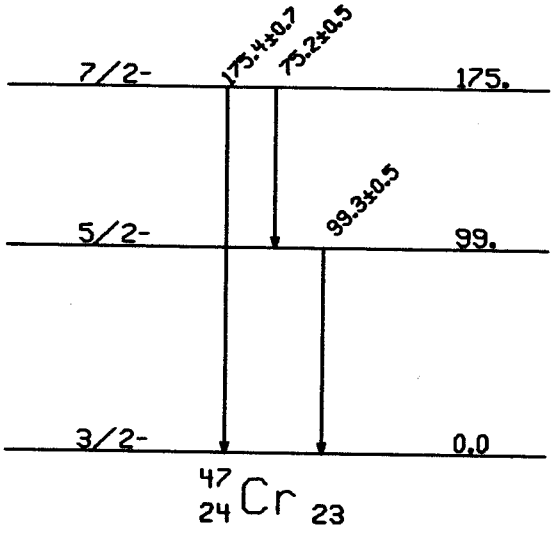

Fig. 2 Proposed ^{47}Cr level scheme from in-beam γ-ray spectroscopy.

REFERENCES

1. D. Mueller, Ph.D. Thesis, Michigan State University, June, 1976.

2. M.D. Edmiston, R.A. Warner, Wm.C. McHarris, and W.H. Kelly, Proceedings of the Third International Conference on Nuclei Far From β Stability, Cargese, Corsica, 1976.

3. J.C. Hardy and I.S. Towner, Phys. Lett. 58B, 261(1975).

4. M. Blann and F. Plasil, Nuclear evaporation code ALICE adapted for the MSU Cyclotron Laboratory Sigma-7 computer by W. Bentley.

Gamma-Ray Studies of ^{93}Ru Decay

M. Distasio, Wm. C. McHarris, R. Firestone, and R. Warner

Recently our work has centered on the odd mass N=49 isotones, in particular ^{93}Ru. By applying the model used by Auerbach and Talmi,[1] ^{93}Ru is assumed to have an inert core of 38 protones in the $p_{1/2}$ and $g_{1/2}$ shell-model orbitals. This together with one hole in the N=50 closed shell leads to the prediction of two low-lying states with configurations of $\pi(^1g_{9/2})^4_{j=0} \times \nu(^1g_{9/2})^{-1}_{j-9/2}$ and $\pi(^1g_{9/2})^4_{j=0} \times \nu(^1p_{1/2})^{-1}_{j=1/2}$. Moreover ^{93}Ru is of special interest, being the heaviest known member of this N=49 isotone series, the other members of which have manifested systematics in good qualitative agreement with simple shell-model predictions. Up through A=91 all the members of this series have been shown experimentally to have a $9/2^+$ ground state and a $1/2^-$ first excited state with an energy spacing between the two levels that increases with increasing atomic number.[2] The low-lying level structure is still unproven but it appears hopeful that we will be able to extend the aforementioned trends to the case of ^{93}Ru. Since there is so little known about ^{93}Ru, it seems that a reasonable approach to the investigation of ^{93}Ru is to study the levels in the nucleus ^{93}Tc fed by the ε/β^+ decay of ^{93}Ru, with the aim of using this knowledge later, in characterizing the levels in the ^{93}Ru nucleus.

Our first experiment with ^{93}Ru was an excitation function run using α-particle beams with the energies 40, 44, and 48 MeV. The excitation function for ^{93}Ru was obtained by following the prompt 680 keV transition in ^{93}Ru fed by the ε/β^+ decay of ^{93}Ru. This was used to determine the optimum conditions for producing the ^{93}Ru by the reaction ^{92}Mo(α,3n)^{93}Ru. From this experiment we were then able to determine the feasibility of a half-life measurement of the $9/2^+$ state of ^{93}Ru. A 48 MeV α-beam on the same ^{92}Mo target was chosen for the half-life determination. The data was collected using the MSU Σ-7 task HYDRA.[3] This task allows the routing of addresses from one ADC into seven consecutive spectra. This experiment yielded a half-life of 54±2 sec for the ^{93}Ru $9/2^+$ state, in good agreement with the results reported by Doron and Lanford.[4]

Finally, a γ-γ coincidence experiment, using two Ge(Li) detectors was performed using the same reaction and beam energy. Data were recorded with the acquisition task IIEVENT.[3] An example of some of the data taken in this coincidence run is shown in Fig. 1. This is the integral spectrum obtained with an ORTEC 18%* Ge(Li) detector. Our results up to this point, in conjunction with those from ^{92}Mo(p,γ)^{93}Tc and numerous charged-particle reaction experiments[5] leads to the tentative decay scheme in Fig. 2.

*18% efficient at 1332 keV relative to a 3x3 inch NaI crystal at 10 inches. Resolution 2.1 keV at ^{60}Co 1332 keV line.

REFERENCES

1. N. Auerbach and I. Talmi, Nucl. Phys. 64, 458 (1965).
2. C.M. Lederer, J.M. Hollander, and I. Perlman, Table of Isotopes, Sixth edition (1967), Wiley Interscience Publisher.
3. R. Au, Michigan State University Cyclotron Laboratory, unpublished.
4. T. Doron and W. Lanford, J. Inorg. Nucl. Chem. 34, 443 (1973).
5. Nuclear Data Sheets, Vol. 8, No. 6 (1973).

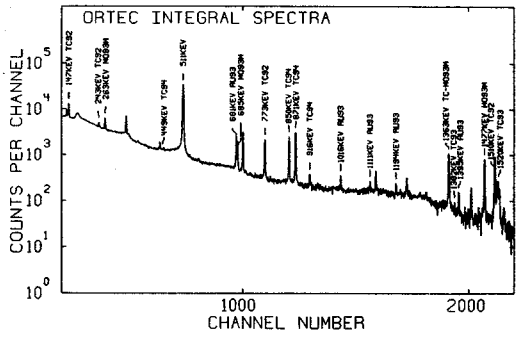

Fig. 1.--Portion of integral spectra from γ-γ coincidence.

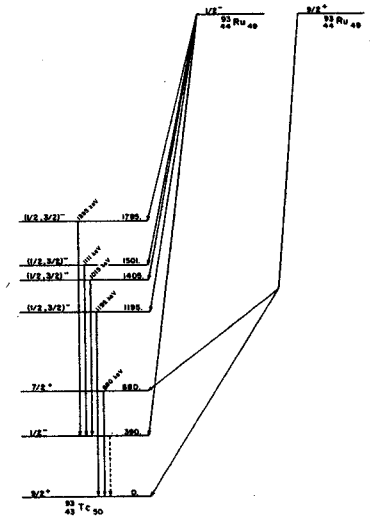

Fig. 2.--Decay of ^{93}Ru to levels in ^{93}Tc.

Gamma Ray Studies of the Decay of ^{115}Te

D.C. Coyle, R.A. Warner, R.B. Firestone, Wm.C. McHarris, and W.H. Kelly

Our experimental group has had a strong interest in study Sb isotopes using primarily in-beam γ-ray techniques.[1,2] Because of the ease in studying short-lived activities with our Helium-Jet-Recoil-Transport System,[3] energy levels in ^{115}Sb could be studied from the short-lived β^+ decay of the ^{115}Te. A SnO_2 target enriched to 95% ^{116}Sn was supported on a 0.05 mm Al foil backing, and a 70 MeV τ beam was degraded to 40 MeV with Al absorbers to optimize ^{115}Te production. As described elsewhere,[3] the activity was transported to a low background counting area with a helium jet system where it was counted with Ge(Li) detectors.

Using the computer program HYDRA,[4] a series of six 6-minute spectra were recorded. The code POLYBAND[5] was used to obtain half-lives with errors for the strongest ^{115}Sb γ-rays measured in this experiment. These results are displayed in Table 1. Charvet et al.[6] report two isomers of ^{115}Te with half-lives of 6.0 and 7.5 minutes; however, we cannot so far confirm all their findings. The weighted average half-life for these 7 transitions is 5.76±0.09 minutes, in agreement with the shorter-lived isotope observed by Charvet et al.[6]

Table 1 Half-Lives of the most prominent ^{115}Sb γ-Rays

γ Energies (keV)	$t_{1/2}$ (min.)
602	5.9 ± 0.2
656	5.5 ± 0.6
723	5.8 ± 0.2
1098	5.7 ± 0.2
1326	5.7 ± 0.2
1380	5.7 ± 0.2
1600	5.8 ± 0.4

γ-γ coincidence experiments were also performed using Ge(Li) detectors (ORTEC 18% and EDAX). The most prominent gates are listed in Table 2. The relative half-lives and γ-γ coincidence data support the assignments for all but the weaker γ-transitions seen by Charvet et al[6] and Shilin and Burmistrov.[7] Our most reliable assignments are shown in Table 3.

Using the computer code ALICE,[8] which calculates cross sections for compound nuclear reactions, we confirm that there are other strong competing reactions through the 35 MeV to 45 MeV beam energy range. The major impurities identified are ^{116}Te, ^{117}Te, ^{115}Sb and their decay porducts. The $^{116}_{50}Sn(\tau,4n)^{115}_{52}Te$ reaction cross section changes slowly over this range as is calculated by ALICE and shown by an experimental excitation function taken at 35 MeV, 40 MeV, and 45 MeV τ beam energies. Unfortunately, the same appears true for the competing reactions. Further experiments involving fast chemistry and optimizing counting intervals in order to avoid contaminants are in progress.

Table 2 Best γ-γ Coincidence Gates

γ Gates (keV)	γ Coincidence Gates
374	567, 1380, annihilation
428	723, annihilation
567	374, 428, 472, 723, annihilation
656	428, 723, annihilation
723	602, 656, 1012, 1600, annihilation
1098	1295, annihilation
1380	567, 944, annihilation
1600	723, annihilation

Table 3 Assignment of ^{115}Sb γ-rays

Energy (keV)	Relative Intensity	Energy (keV)	Relative Intensity
374	20	944	4
428	6	996	4
567	12	1012	4
602	15	1098	38
656	23	1326	42
723	100	1380	44
770	7	1600	5
923	--		

REFERENCES

1. See articles on these isotopes elsewhere in this report.

2. C.B. Morgan, "States in ^{116}Sb from ^{116}Te Decay and ^{116}Sn (p, nγ)^{116}Sb", Ph.D. Thesis, Michigan State University (1975).

3. K.L. Kosanke, M.D. Edmiston, R.A. Warner, R.B. Firestone, and Wm. C. McHarris, Nucl. Inst. Meth. 17, 78 (1975).

4. R. Au, HYDRA, Michigan State University Cyclotron Laboratory Sigma-7 Program Description Book.

5. S. Faber, POLYBAND: A Least Squares Routine, unpublished.

6. A. Charvet, R. Chery, D. Huu Phuoc, R. Duffait, and M. Morgue, J. Phys. (Paris) 35, 806 (1974).

7. V.A. Shilin and V.R. Burmistrov, Ser Fiz 36, 2509 (1972).

8. M. Blann and F. Plasil, ALICE: A Nuclear Evaporation Code, U.S. Atomic Energy Commission Report No. COO-3494-10, 1973.

Excited States in ^{117}Sb Via the (p,xnγ) Reactions

K. Shafer,* J.A. Carr, W.H. Kelly, Wm. C. McHarris, and R.A. Warner

Antimony nuclei, with one proton outside the Z=50 closed shell, should be particular simple nuclei to study. This discussion summarizes the results of a series of in-beam gamma-ray and conversion electron experiments which have been conducted in the investigation of the level structure of ^{117}Sb by means of the ^{117}Sn(p,nγ)^{117}Sb and ^{120}Sn(p,4nγ)^{117}Sb reactions. These include gamma-ray singles and coincidence measurements, angular distributions, and gamma-ray excitation function measurements. In all of these experiments large volume, high resolution Ge(Li) detectors were used for the detection of the gamma-rays.

Gamma-ray singles data were taken while bombarding a self-supporting foil of ^{117}Sn with proton beams at incident energies of 6, 10, and 12.5 MeV. The target material was enriched to about 80% ^{117}Sn and the target thickness was approximately 700 μg/cm^2. Most of the data were taken with the 6 MeV protons. Good energy calibrations were achieved by simultaneously counting gamma-rays from an NBS composite standard source and from ^{117}Sb. The resulting spectrum was analyzed using the peak-fitting computer code SAMPO. Energies for the ^{117}Sb peaks were obtained by making a polynomial fit to the well known energies of the NBS peaks.

Gamma-gamma coincidence data were taken using two Ge(Li) detectors with the addresses of the coincident events being stored serially on magnetic tape for off-line analysis of a later time. These data, along with good energy and relative intensity information, made it possible to sort out and properly order level sequences and gamma-ray cascades in the ^{117}Sb decay scheme (Fig. 1). A total of 37 gamma-rays and 17 levels were added to the previously known structure[1] of ^{117}Sb from the results of this experiment.

Spin assignments were made to some of these levels based on the results of the angular distribution experiment. Gamma-ray angular distribution measurements were made in random order at angles of 90°, 105°, 115°, 125°, 135°, 145°, and 155° with normalization being provided by counting elastically scattered protons with a Si surface barrier detector. The data were fit to the equation

$$W(\theta) = 1 + A_2P_2(\cos\theta) + A_4P_4(\cos\theta)$$

to obtain experimental A_2 and A_4 values. Transition multipolarities and spins were then deduced.

Support for several of the spin assignments made as a result of the angular distributions was gained from the excitation function experiment. In this experiment gamma-ray intensities from the ^{120}Sn(p,4nγ)^{117}Sb reaction were measured by bombarding a 9.9-mg/cm^2 target of ^{120}Sn with protons at energies of 35, 38, 40, and 45 MeV. Spins of the various levels were determined by plotting the relative intensities of the gamma-rays as a function of energy. Unfortunately, the presence of numerous gamma-rays from competing reactions made the excitation data somewhat less definitive than the angular distribution results. Coincidence experiments are yet to be performed with the (p,4nγ) reaction.

References

1. G. Berzins, W.H. Kelly, G. Graeffe, and W.B. Walters, Nucl. Phys. A104,241(1967).

*Current address: Fermilab, Batavia, IL 60510.

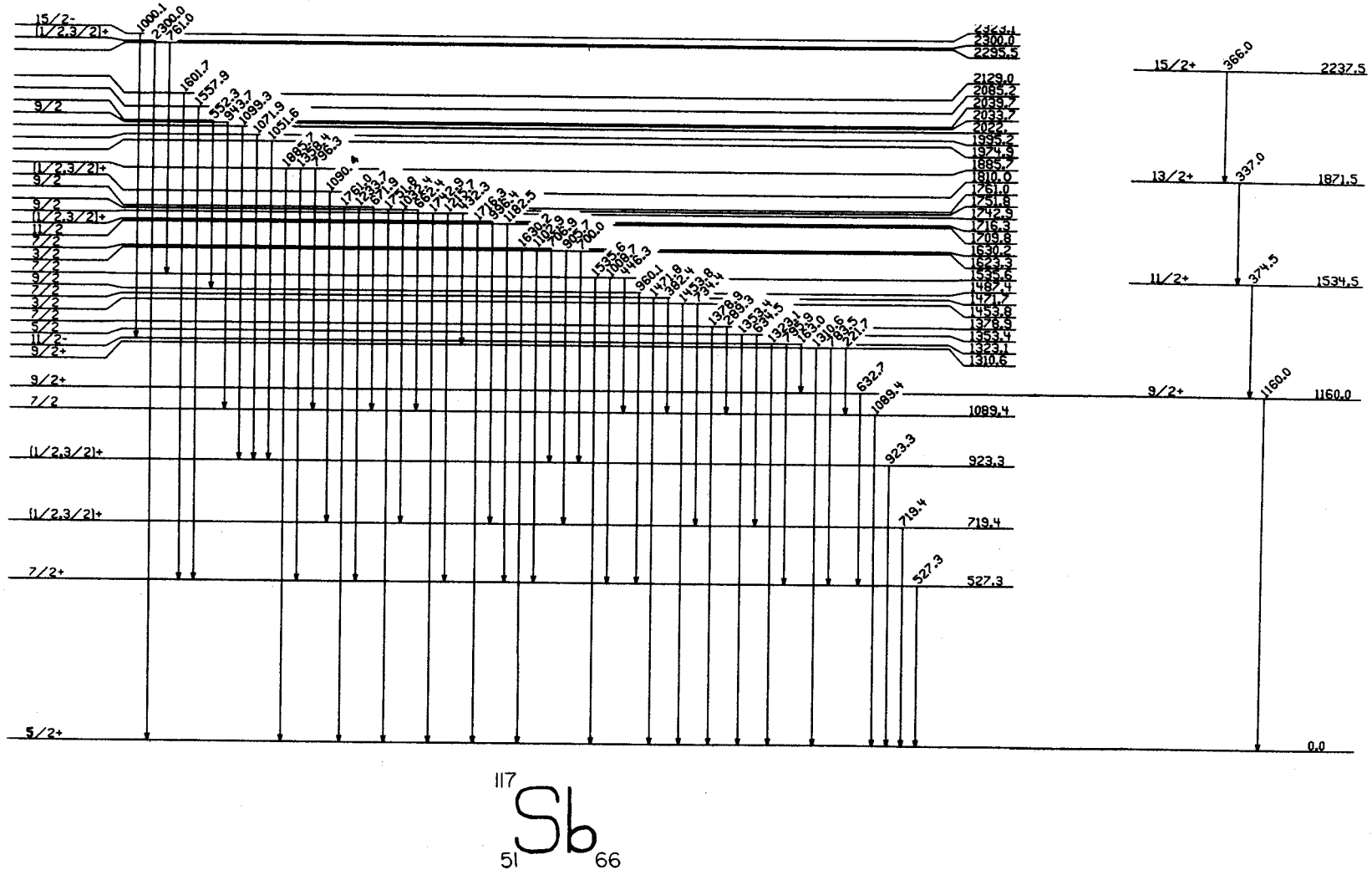

$^{117}_{51}Sb_{66}$

FIG. 1.--Preliminary Decay Scheme of ^{117}Sb.

Gamma Ray Spectroscopy of the Odd-A Nucleus ^{119}Sb

J.A. Carr, K. Shafer, R.A. Warner, Wm. C. McHarris and W.H. Kelly

The nucleus of ^{119}Sb was studied extensively several years ago by the beta decay of ^{119}Te[1,2] and by the (^{3}He,d) reaction.[3] These results were accurate for the low lying states, but incomplete at excitations above ~1.2 MeV. With the advent of larger-volume high resolution γ-ray detectors and computer assisted analysis of mega-channel coincidence data, the study of low-spin excited states of these nuclei (where there is a high level density) can be attempted with greater confidence.

In the current study, the levels were studied by observing the γ-rays following the ^{119}Sn(p,nγ) reaction at 10 MeV, and the ^{122}Sn(p,4nγ) reaction at 40 MeV. The latter reaction was used in order to transfer more angular momentum to examine the "rotational" band built on the 971 keV 9/2$^+$ state.[4] In both cases the targets were ~1 mg/cm^2 self-supporting foils of the enriched isotopes so that competing reactions were not a serious problem.

We took γ-γ coincidence data. The spectra of those γ-rays coincident with events in particular gates were extracted and studied. The decay scheme in Fig. 1 resulted. One notes that many low-spin states, as well as the "rotational" band, were populated at this low energy.

The γ-rays were observed using large Ge(Li) detectors and the spectra analysed with the Σ-7 computer using the peak analysis code SAMPO. The energies, intensities and angular distributions of the γ-rays were measured with the 10 MeV reaction. The angular distributions were normalized using elastically scattered protons observed by a surface barrier detector. The strongest transitions gave reasonably unambiguous results, and these were used to assign the spins of the levels in Fig. 1.

We extended these experiments to include larger angular momentum. The code ALICE[5] was run to determine the optimal energy for the (p,4nγ) reaction, and spectra were taken at 35, 38, 40 and 45 MeV proton energies to study the excitation function of the transitions in ^{119}Sb. This allowed a more rational choice of the optimum beam energy, as well as providing additional information to check some of the spin assignments. The plot in Fig. 2 demonstrates the spin dependence of the excitation of these levels. The data in Fig. 2 were normalized to the intensity of the 270 keV γ-ray and scaled to the same point at 35 MeV.

A γ-γ coincidence experiment was performed using 45 MeV protons with the HeJRT system[6] to study the transitions out of the isomeric state reported recently.[7] A decay scheme incorporating the results is not yet complete. However, we can report that we see what resembles a band built on the 1366 keV 11/2$^-$ level with 947 and 237 keV γ-rays from levels with spins 15/2$^-$ and 19/2$^-$ respectively, as well as a 135 keV crossover from the 19/2$^-$ level to the 2419 keV 17/2$^+$ level.

When one takes in the broad view of what we have learned thus far, one is immediately struck by the density, complexity and diversity of the levels populated by this reaction. This often makes it desirable to use different tools to probe the different aspects of these nuclear levels. The results obtained here will be combined with some recent beta decay results,[8] (p,α) work,[9] and the heavy ion work[4,7] to obtain more insight into the nature of this very interesting nucleus.

References

1. G. Berzins and W.H. Kelly, Nucl. Phys. A92, 65(1967).
2. G. Graeffe, E.J. Hoffman and D.G. Sarantites, Phys. Rev. 158,1183(1967).
3. T. Ishimatsu, K. Yagi, H. Ohmura, Y. Nakajima, T. Nakagawa and H. Orikara, Nucl. Phys. A104, 481(1967).
4. A.K. Gaigalas, R.E. Shroy, G. Schatz and D. B. Fossan, Phys. Rev. Lett. 35,555(1975).
5. M. Blann and F. Plasil, an unpublished nuclear evaporation code.
6. K. L. Kosanke, MSU Thesis (1973).
7. A.K. Gaigalas, et al., private communication.
8. R.A. Meyer, et al., private communication.
9. See the ^{122}Te(p,α) article in this report.

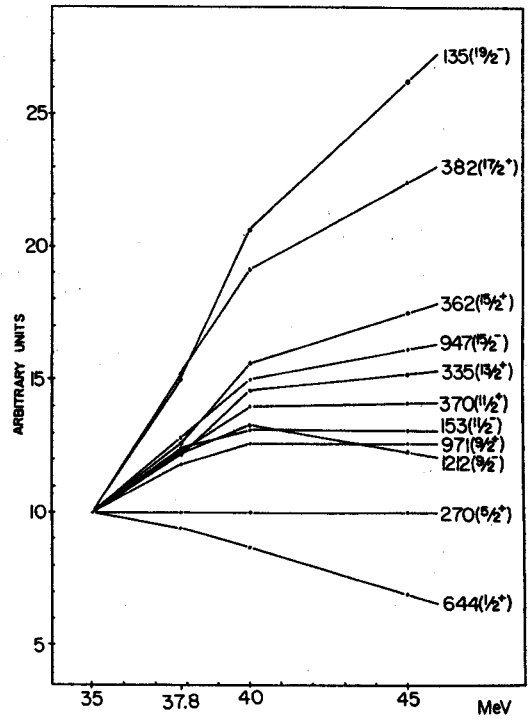

Fig. 2 Excitation function of levels in ^{119}Sb, normalized as described in the text. The γ-ray energies are given in keV, along with the spin of the level being depopulated.

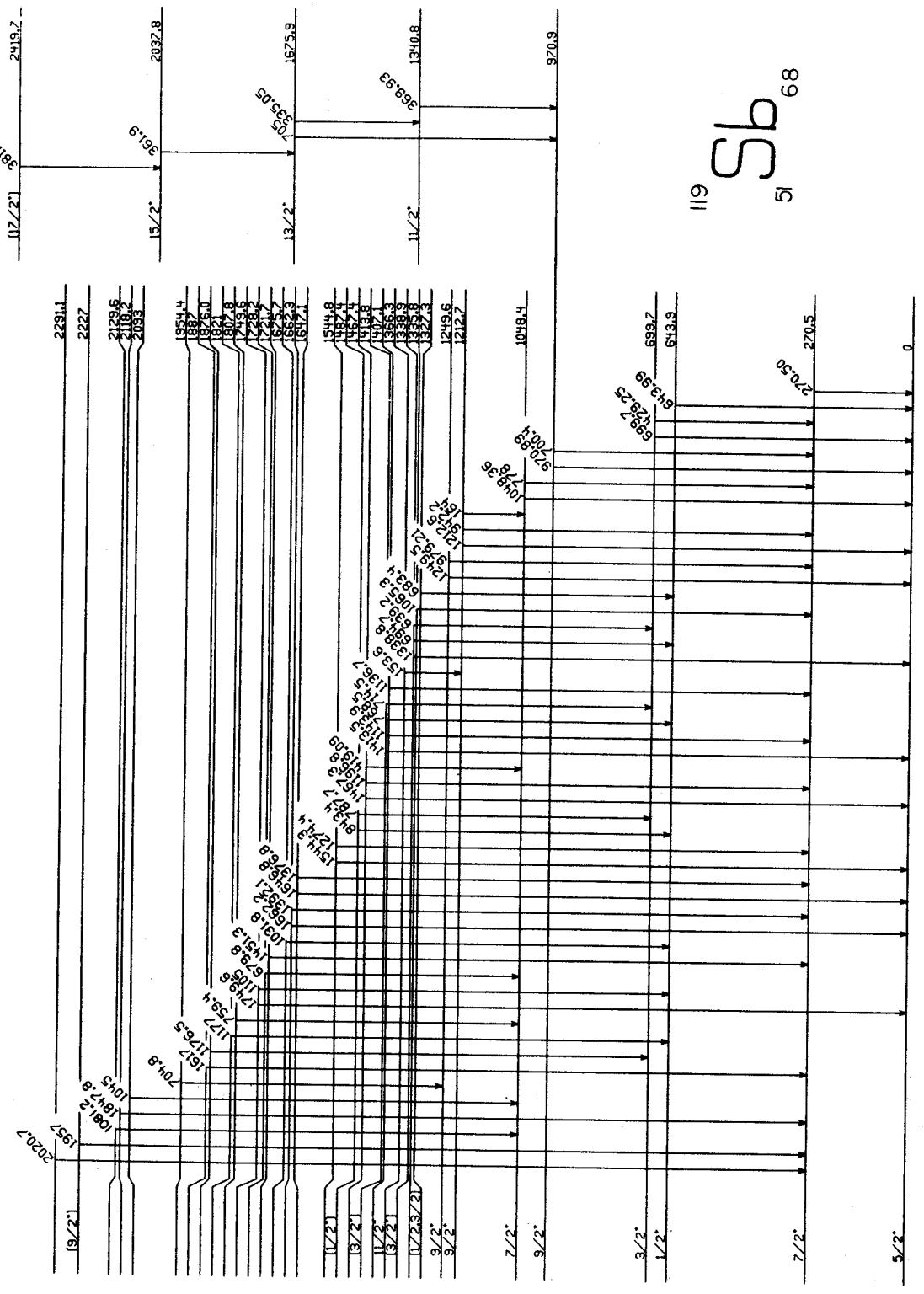

Fig. 1.--Decay scheme obtained from $^{119}Sn(p,n\gamma)^{119}Sb$ at 10 MeV.